



Published in final edited form as:

J Nat Prod. 2018 January 26; 81(1): 188–202. doi:10.1021/acs.jnatprod.7b00876.

Isolation, Derivative Synthesis, and Structure-Activity Relationships of Anti-Parasitic Bromopyrrole Alkaloids from the Marine Sponge *Tedania brasiliensis*[#]

Lizbeth L. L. Parra^{†,‡,#}, Ariane F. Bertonha^{†,§,#}, Ivan R. M. Severo[†], Anna C. C. Aguiar[⊥], Guilherme E. de Souza[⊥], Glaucius Oliva[⊥], Rafael V. C. Guido[⊥], Nathalia Grazzia^{||}, Tábata R. Costa^{||}, Danilo C. Miguel^{||}, Fernanda R. Gadelha^{||}, Antonio G. Ferreira[∇], Eduardo Hajdu[○], Daniel Romo^{§,*}, and Roberto G. S. Berlinck^{†,*}

[†]Instituto de Química de São Carlos, Universidade de São Paulo, CP 780, CEP 13560-970, São Carlos, SP, Brazil

[§]Department of Chemistry & Biochemistry, Baylor University, Waco, TX 76706, USA

[⊥]Instituto de Física de São Carlos, Av. Joao Dagnone, 1100, Jardim Santa Angelina, São Carlos, SP, 13563-120, Brazil

^{||}Departamento de Biologia Animal e Departamento de Bioquímica e Biologia Tecidual, Instituto de Biologia, Universidade Estadual de Campinas, CEP 13083-862, Campinas, SP, Brazil

[∇]Departamento de Química, Universidade Federal de São Carlos, Rod. Washington Luiz, km 235 - SP-310, CEP 13565-905, São Carlos, SP, Brazil

[○]Museu Nacional, Universidade Federal do Rio de Janeiro, Quinta da Boa Vista, s/n, CEP 20940-040, Rio de Janeiro, RJ, Brazil

Abstract

The isolation and identification of a series of new pseudoceratidine (**1**) derivatives from the sponge *Tedania brasiliensis* enabled the evaluation of their anti-parasitic activity against *Plasmodium falciparum*, *Leishmania (Leishmania) amazonensis*, *Leishmania (Leishmania) infantum* and *Trypanosoma cruzi*, the causative agents of malaria, cutaneous leishmaniasis, visceral leishmaniasis and Chagas disease, respectively. The new 3-debromopseudoceratidine (**4**), 20-debromopseudoceratidine (**5**), 4-bromopseudoceratidine (**6**), 19-bromopseudoceratidine (**7**) and 4,19-dibromopseudoceratidine (**8**) are reported. New tedamides A – D (**9** – **12**), with an unprecedented 4-bromo-4-methoxy-5-oxo-4,5-dihydro-1*H*-pyrrole-2-carboxamide moiety, are also described. Compounds **4** and **5**, **6** and **7**, **9** and **10**, and **11** and **12** have been isolated as pairs of

[#]Dedicated to Prof. Raymond J. Andersen, for his outstanding contributions to the chemistry of natural products.

^{*}Corresponding Author: Tel: +55-16-33739954; Fax: +55-16-33739952; rgsberlinck@iqsc.usp.br, ORCID: 000-0001-8883-6897.

[‡]Present address: Departamento de Química, Universidad Santiago de Cali, Calle 5#62-00, Santiago de Cali, Valle del Cauca, Colombia.

[#]These authors contributed equally.

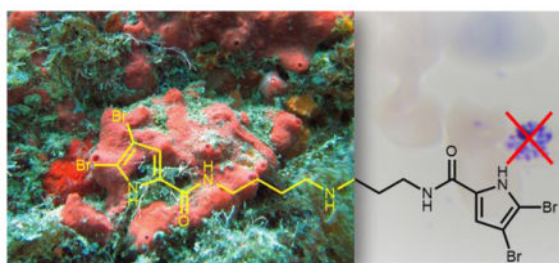
Supporting Information

The Supporting Information is available free of charge on the ACS Publications website at DOI:

Isolation procedures, HRMS, IR, ¹H and ¹³C NMR spectra of compounds **1-12**, synthesis procedures and IR, HRMS, ¹H and ¹³C NMR spectra of compounds **16, 17, 20, 21, 23, 25, 27 – 29, 31, 33, 35, 38, 39, 42, 43, 46, 47, 50** and **51**.

inseparable structural isomers differing in their sites of bromination or oxidation. Tedamides **9+10** and **11+12** were obtained as optically active pairs, indicating an enzymatic formation rather than an artefactual origin. *N*^{1,2}-Acetyl pseudoceratidine (**2**) and *N*^{1,2}-formyl pseudoceratidine (**3**) were obtained by derivatization of pseudoceratidine (**1**). The anti-parasitic activity of pseudoceratidine (**1**) led us to synthesize 23 derivatives (**16, 17, 20, 21, 23, 25, 27 – 29, 31, 33, 35, 38, 39, 42, 43, 46, 47, 50** and **51**) with variations in the polyamine chain and aromatic moiety in sufficient amounts for biological evaluation in anti-parasitic assays. The measured anti-malarial activity of pseudoceratidine (**1**) and derivatives **4, 5, 16, 23, 25, 31** and **50** provided an initial SAR evaluation of these compounds as potential leads for anti-parasitics against *Leishmania* amastigotes and against *Plasmodium falciparum*. The results obtained indicate that pseudoceratidine represents a promising scaffold for the development of new anti-malarial drugs.

Graphical Abstract



Bromopyrrole alkaloids isolated from marine sponges encompass a remarkable chemical diversity of potentially bioactive compounds. These metabolites range from oroidin-related archetypal motifs to structurally complex oroidin-tetramers, the stylissadines.^{1–3} Such alkaloids are prevalent in sponges belonging to the order Agelasida (particularly within the genus *Agelas*, family Agelasidae).^{1–3} Nevertheless, several of these alkaloids have also been found in sponges of the genera *Axinella* (Axinellidae, Halichondrida), *Axinyssa* (Halichondriidae, Halichondrida), *Callyspongia* (Callyspongiidae, Haplosclerida), *Eurypon* (Raspailiidae, Poecilosclerida), *Homaxinella* (Suberitidae, Hadromerida), *Hymeniacion* (Halichondriidae, Halichondrida) and *Stylissa* (Halichondriidae, Halichondrida).^{1–7} Therefore, past assumptions on the character of bromopyrrole alkaloids as chemotaxonomical markers of these sponges^{4–7} are now challenged by their more widespread occurrence. Such is also the case for our present isolation of pseudoceratidine (**1**) derivatives from the marine sponge *Tedania brasiliensis* (Tedaniidae, Poecilosclerida).

Pseudoceratidine (**1**) was previously isolated solely from the sponge *Pseudoceratina purpurea* (Pseudoceratinidae, Verongida).^{8,9} The compound displayed more potent anti-fouling activity than its mono-substituted 4,5-dibromo-1*H*-pyrrole-2-carboxylic acid spermidine analogs.¹⁰ In these previous studies, it was found that both the substitution pattern of the terminal rings and the length of the triamine chain of pseudoceratidine derivatives affect the anti-fouling activity. Furthermore, pseudoceratidine also displayed the most potent antibacterial activity against *Staphylococcus aureus*, *Listeria monocytogenes*, *Pseudomonas aeruginosa*, *Escherichia coli* and *Serratia liquefaciens*.¹¹ In the present investigation, we report the anti-parasitic activity of pseudoceratidine and several new

synthetic pseudoceratidine derivatives against *Plasmodium falciparum*, *Leishmania (Leishmania) amazonensis*, *L. (L.) infantum* and *Trypanosoma cruzi*.

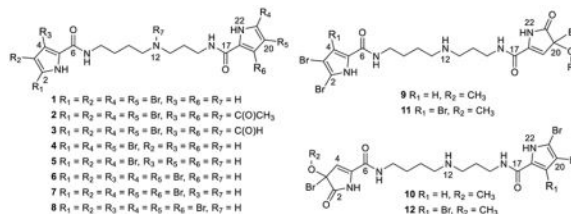
Malaria, caused by *Plasmodium* spp., is among the most devastating vector-borne human infectious diseases. It is estimated that over 3.4 billion people worldwide are at risk of infection. Malaria is prevalent in tropical and sub-tropical regions, affecting 212 million people and causing 429,000 deaths in 2015. In Africa, *P. falciparum* is responsible for the highest mortality rate of children under 5 years of age. Malaria etiologic agents have developed resistance to several antimalarial drugs, including emerging resistance to artemisinin and artemisinin-based combination therapies that comprise current first-line treatments.¹² Thus, the discovery of new antimalarial lead compounds is of utmost importance.

Leishmaniasis is a group of diseases caused by several species of protozoan parasites belonging to the genus *Leishmania* endemic in more than 80 countries.¹³ Transmitted by different sandfly species, *Leishmania* parasites infect cells from the mononuclear phagocytic system leading to clinical manifestations that vary from localized, disseminated and diffuse skin lesions (cutaneous leishmaniasis) to a systemic multi-organ infection (visceral leishmaniasis). Visceral leishmaniasis is fatal if left untreated. Treatment options are limited to parenteral drugs, including pentavalent antimonials as the first-line drugs, which very often presents severe side effects. The utilization of liposomal amphotericin B and oral miltefosine proved useful for treating patients with visceral leishmaniasis. Nevertheless, the high cost of liposomal amphotericin B and the miltefosine teratogenic effect, in addition to its long half-life, hampers the therapeutic success of such treatments.^{14,15} Therefore, the identification of new drug candidates for leishmaniasis treatment remains imperative in the current therapeutic scenario.

Trypanosoma cruzi is the causative agent of Chagas disease, which may lead to fatal disorders such as cardiomegaly and megacolon in approximately 30% of patients.¹⁶ The disease is an emerging health issue in North America and Europe.^{17–19} Approximately 8–10 million people in Latin American countries are infected by *T. cruzi*, with an annual death rate of approximately 14,000 people.^{18,19} Benznidazole, toxic and of limited efficacy, is the only available therapy in Brazil for Chagas disease. No effective treatment exists for chronic phase patients affected by Chagas disease.²⁰ Thus, the discovery of new therapies for Chagas disease is sorely needed. Furthermore, there are no approved vaccines for the treatment of humans to prevent malaria, leishmaniasis or Chagas disease.

In our continuing search for anti-parasitic marine metabolites,^{21–24} we verified that the MeOH anti-parasitic extract of *T. brasiliensis* contained pseudoceratidine (**1**) as the most abundant metabolite. Related minor constituents were detected only by HPLC-UV-MS because of the high abundance of **1** in the sponge extract. Several chromatographic separations of this extract yielded a series of minor pseudoceratidine derivatives. These include the new tedamides A – D (**9** – **12**), along with the new 3-debromopseudoceratidine (**4**), 20-debromopseudoceratidine (**5**), 4-bromopseudoceratidine (**6**), 19-bromopseudoceratidine (**7**) and 4,19-dibromopseudoceratidine (**8**). Compounds **4** and **5**, **6** and **7**, **9** and **10**, as well as **11** and **12** have been isolated as pairs of inseparable structural

isomers differing in their sites of bromination or oxidation. Since pseudoceratidine displayed good anti-*P. falciparum* activity, we prepared a series of pseudoceratidine derivatives with different polyamine and aromatic moieties, aiming to assess their anti-*Plasmodium falciparum*, anti-*Leishmania* spp. and anti-*T. cruzi* activities and begin evaluation of their structure-activity relationships.



RESULTS AND DISCUSSION

Isolation and Identification of Natural Pseudoceratidine Derivatives

Analysis of the HRMS and NMR data of **1**^{8,9} facilitated the identification of minor pseudoceratidine congeners **4** – **12** (Tables 1 – 4) that were all isolated as their formate salts. The inseparable mixture of 3-debromopseudoceratidine (**4**) and 20-debromopseudoceratidine (**5**) displayed a protonated molecule cluster at m/z 565.9409/567.9389/569.9370/571.9354 with peaks showing relative intensities of 1:3:3:1. The $[M+H]^+$ ion at m/z 565.9409 corresponded to the formula $C_{17}H_{23}^{79}Br_3N_5O_2$, with one fewer bromine atom and one more hydrogen atom than **1**. Monobromo substitution at one of the pyrrole moieties was verified in the COSY spectrum of **4** and **5**. Coupling between two hydrogens was observed in one of the pyrrole rings, at δ_H 6.11 (dd, $J = 2.5$ and 3.7 Hz, H-4 or H-19) and at δ_H 6.71/6.72 (dd, $J = 2.5$ and 2.7 Hz, H-3 or H-20), both of which coupled with an NH group at δ_H 12.13/12.18 (br s). A doublet at δ_H 6.89/6.90 (d, $J = 2.2$ Hz, H-4 or H-19) was assigned to the hydrogen of a 2,3-dibromosubstituted pyrrole group, which coupled only to the NH group at δ_H 12.67/12.63 (d, $J = 2.2$ Hz). Analysis of the COSY spectrum of **4** indicated that H-4 (δ_H 6.11, dd, $J = 2.5$ and 3.7 Hz) was vicinal to H-3 (δ_H 6.72 (dd, $J = 2.5$ and 2.7 Hz). In the HMBC spectrum, H-4 coupled with C-2 (δ_C 102.7), C-5 (δ_C 128.4) and C-6 (δ_C 159.9), whereas NH-7 (δ_H 8.03, t, $J = 5.7$ Hz) coupled with C-6 and C-8 (δ_C 38.0). These couplings indicated that in **4** the monobromopyrrole-2-carboxylic acid group was attached to the NH amide connected to the four-methylene moiety of spermidine, because H₂-8 showed couplings to H₂-9 in the COSY spectrum and to C-9 and C-10 in the HMBC spectrum. Considering the NMR data of **4**, the dibromopyrrole-2-carboxylic acid group had to be attached to the three-methylene moiety of spermidine. Indeed, H-19 (δ_H 6.90, d, $J = 2.2$ Hz) coupled with C-18 (δ_C 128.1) and with C-21 (δ_C 104.9), whereas NH-16 (δ_H 8.24, t, $J = 6.0$ Hz) coupled with C-15 (δ_C 36.0) and C-17 (δ_C 159.1). In the HMBC spectrum, the isomeric compound **5** shows H-4 (δ_H 6.89, d, $J = 2.2$ Hz) at the dibromopyrrolecarboxylic acid group coupling with C-2 (δ_C 104.7), C-5 (δ_C 128.0) and C-6 (δ_C 159.4), whereas NH-7 (δ_H 8.14, t, $J = 5.7$ Hz) coupled with C-6 at δ_C 159.4 and with C-8 (δ_C 37.9). At the other end of the spermidine chain of **5**, H-19 (δ_H 6.13, dd, $J = 2.2$ and 3.7 Hz) showed a coupling with H-20 (δ_H 6.71, dd, $J = 2.5$ and 2.7 Hz) in the COSY spectrum and coupled with C-18 (δ_C 128.3) and with C-21 (δ_C 102.4) in the HMBC

spectrum. Unambiguous ^1H and ^{13}C assignments were also based on the relative integration of the ^1H signals of **4** and **5**, those of **4** being slightly higher than those of **5**, with a relative abundance of approximately 55/45, respectively. The ^1H and ^{13}C signals for the methylene groups of the spermidine chain were essentially the same for **4** and **5** (Tables 1 and 2) and identical to those of **1**. Thus, the structures of 3-debromopseudoceratidine (**4**) and 20-debromopseudoceratidine (**5**) were established.

A fraction presenting an inseparable mixture of the isomeric 4-bromopseudoceratidine (**6**) and 19-bromopseudoceratidine (**7**) was obtained along with one distinct fraction providing pure **7**. Many attempts made to separate both **6** and **7** under different HPLC conditions were unsuccessful. The HRMS spectrum of the mixture of **6** and **7**, as well as that of pure **7**, displayed a protonated molecule cluster at m/z 721.7632/723.7587/725.7626/727.7581/729.7564/731.7520, with peaks showing relative intensities of 1:5:10:10:5:1. The $[\text{M}+\text{H}]^+$ ion at m/z 721.7632 corresponded to the formula $\text{C}_{17}\text{H}_{21}^{79}\text{Br}_5\text{N}_5\text{O}_2$, with one more bromine atom and one fewer hydrogen atom than **1**. The ^1H NMR spectrum of **7** (Table 1) presented a singlet at δ_{H} 6.89 integrating to one ^1H (H-4), indicating that one of the pyrrole moieties was substituted by three bromines. The HMBC spectrum of **7** showed couplings of H-4 with C-2 (δ_{C} 104.6), C-3 (δ_{C} 97.9, weak), C-5 (δ_{C} 128.3) and C-6 (δ_{C} 159.1), as well as between NH-7 (δ_{H} 8.14, br t, $J = 5.6$ Hz) and C-6 and C-8 (δ_{C} 38.0), which enabled us to establish to which of the two amides the dibrominated pyrrole moiety was attached. Because the H₂-8 methylene protons (δ_{H} 3.21) showed HMBC couplings to C-9 (δ_{C} 26.5) and to C-10 (δ_{C} 23.3), whereas H₂-11 (δ_{H} 2.89) showed couplings to C-10, C-9 and C-13 (δ_{C} 44.7), it was possible to determine the connectivity of the 2,3-dibromopyrrole-5-carboxylic acid group to NH-7 in compound **7**. Additional HMBC couplings between NH-16 (δ_{H} 7.72) and C-17 (δ_{C} 162.0) and C-15 (δ_{C} 35.3), between H₂-15 (δ_{H} 3.25) and C-14 (δ_{C} 26.5) and C-13, along with couplings observed between H₂-13 (δ_{H} 2.86) and C-11, C-14 and C-15, confirmed the structure of 19-bromopseudoceratidine (**7**). Finally, MS/MS analysis of **7** provided further support for its structure (Figures S30 and S31, Supporting Information). Fragment ions detected at m/z 395.0079, 397.0097, 399.0098 (1:2:1) and at m/z 320.9235, 322.9219, 324.9187 (1:2:1) indicated that the dibromopyrrole-2-carboxylic acid group was attached to the four-methylene amine moiety of **7**, whereas fragment ions observed at m/z 498.9012, 500.8963, 502.8913 (1:3:3:1), at m/z 472.9718, 474.9163, 476.9141, 478.9121 (1:3:3:1) and at m/z 384.8184, 386.8165, 388.8146, 390.8121 (1:3:3:1) indicated that the tribromopyrrole-2-carboxylic acid group was attached to the three-methylene amine moiety of **7**, confirming its structure with no ambiguity.

The assignments of ^1H and ^{13}C NMR signals of **6** were also established by analysis of NMR data obtained for the 50/50 mixture of **6** and **7** (Tables 1 and 2). For compound **6**, the singlet at δ_{H} 6.90 (H-19) showed couplings in the HMBC spectrum with C-17 (δ_{C} 159.4), C-18 (δ_{C} 128.3) and C-21 (δ_{C} 104.6). The amide NH-16 (δ_{H} 8.24, t, $J = 5.6$ Hz) showed couplings with C-17 and C-15 (δ_{C} 36.0), whereas CH₂-15 (δ_{H} 3.29) showed couplings with C-17 (δ_{C} 159.4), C-14 (δ_{C} 26.2) and C-13 (δ_{C} 44.9) in the HMBC spectrum. In the COSY spectrum, H₂-15 was coupled with NH-16 and H₂-14 (δ_{H} 1.79), which was sequentially coupled with H₂-13 (δ_{H} 2.90). The remaining four-methylene chain was shown to be attached to the

NH-7/C-6 amide group. Complete assignments of ^1H and ^{13}C resonances of **6** and **7** (Tables 1 and 2) enabled the identification of these pentabrominated alkaloids.

The structure of 4,19-dibromopseudoceratidine (**8**) could be established by HRMS analysis, which showed a protonated molecule cluster at m/z 799.6352/801.6241/803.6213/805.6219/807.6194/809.6263/811.6205 with peaks showing relative intensities of 1:6:15:20:15:6:1. The $[\text{M}+\text{H}]^+$ ion at m/z 799.6352 corresponded to the formula $\text{C}_{17}\text{H}_{20}^{79}\text{Br}_6\text{N}_5\text{O}_2$, with two more bromine atoms and two fewer hydrogen atoms than **1**. Inspection of ^1H NMR data obtained for **8** revealed that it corresponded to the 4,19-dibrominated version of **1**, because no pyrrole hydrogen was detected, whereas the ^1H signals of the spermidine chain remained very similar to the corresponding ^1H signals in compounds **1**–**7**. The same pattern was observed for the ^{13}C NMR signals of **8** (Tables 1 and 2). Therefore, the structure of **8** was established as that of 4,19-dibromopseudoceratidine.

Isomeric tedamides A (**9**) and B (**10**) were isolated as an inseparable mixture and presented a protonated molecule cluster at m/z 611.9452/613.9453/615.9435/617.9399, with peaks showing relative intensities of 1:3:3:1. The $[\text{M}+\text{H}]^+$ ion at m/z 611.9452 corresponded to the formula $\text{C}_{18}\text{H}_{25}^{79}\text{Br}_3\text{N}_5\text{O}_4$, with eight double-bond equivalents. A set of doubled signals in the ^{13}C NMR spectrum (Table 4) indicated the presence of two closely related compounds. Several attempts to separate them by HPLC using different columns and/or solvent mixtures failed. Because the intensities of the ^{13}C NMR signal pairs were not identical, we assumed a mixture of a slightly major isomer (**10**) and a minor one (**9**), in 55:45 relative ratio. The assignments of tedamide B isomer (**10**) were established as follows.

The β,γ -unsaturated lactam moiety in **10** was constructed by analysis of the HMBC spectrum. Correlations between NH-1 (δ_{H} 9.07) and C-2 (δ_{C} 167.1), C-3 (δ_{C} 92.1), C-4 (δ_{C} 144.5) and C-5 (δ_{C} 121.5), between H-4 (δ_{H} 7.30, d, $J = 1.6$ Hz) and C-2, C-3 and C-5, as well as between the methoxy group at δ_{H} 3.17 and C-3 accounted for either one of the two hypothetical lactam moieties, A or B (Figure 1). Fragment B was discarded because the coupling constant observed for H-4 ($J = 1.6$ Hz) agrees with a long-distance ^1H - ^1H coupling rather than for a vicinal ^1H - ^1H coupling between H-4 and NH-1. Moreover, analysis of the 1D NOESY spectrum of the mixture of **9** and **10** showed a strong NOE between H-4 and the methoxy group. The ^{13}C signals of sp^2 carbons of **9** and **10** were assigned to a 2,3-dibromopyrrole moiety by comparison with data for **1**.⁸ ^1H and ^{13}C NMR assignments of the spermidine chain were based on the higher intensity of the ^{13}C NMR signals of **10**, by analysis of COSY and HMBC spectra as well as by comparison with data for **1**. Because ^{13}C chemical shifts of the pyrrole conjugated amide carbons lie below δ_{C} 160, for tedamide B (**10**) C-6 was assigned at δ_{C} 165.6 and C-17 at δ_{C} 159.3. Couplings of NH-16 (δ_{H} 8.25) with C-17 and C-15 (δ_{C} 35.9) and of NH-7 (δ_{H} 8.28) with C-6 and C-8 (δ_{C} 38.7) confirmed such assignments (Tables 3 and 4). Analogous reasoning enabled the identification of tedamide A (**9**) as the minor isomer of **10**.

Tedamides C (**11**) and D (**12**) were also isolated as inseparable isomers in a ratio of approximately 28:72, presenting a protonated molecule cluster at m/z 689.8571/691.8551/693.8535/695.8514/697.8499 with peaks showing relative intensities of 1:4:6:4:1. The $[\text{M}+\text{H}]^+$ ion at m/z 689.8571 corresponded to the formula $\text{C}_{18}\text{H}_{24}^{79}\text{Br}_4\text{N}_5\text{O}_4$,

with one more bromine atom than tedamides A and B. Analysis of the NMR data of **11** and **12** indicated that the hydrogen at the pyrrole moiety was missing, whereas the remaining structures were essentially identical to those of compounds **9** and **10** (Tables 3 and 4). Thus, the structures of tedamides **11** and **12** were assigned as those corresponding to the tribrominated pyrrole derivatives of **9** and **10**.

α -Bromo- α -alkoxyamides are known stable chemical entities, frequently utilized as functionalized substrates suitable for the preparation of further derivatives in medicinal chemistry.^{25–30} However, we have been unable to find β,γ -unsaturated- α -bromo- α -alkoxy lactams in the literature or any natural product bearing such functionalities in the SciFinder, Dictionary of Natural Products or MarinLit natural products databases. Thus, the 4-bromo-4-methoxy-5-oxo-4,5-dihydro-1*H*-pyrrole-2-carboxamide moieties of tedamides A and B are structurally unprecedented. Although an artifactual origin could be in principle considered for tedamides given that MeOH was used in the extraction solvent, the mixture of compounds **9** and **10** displayed some optical activity ($[\alpha]_D -7.75^\circ$ (*c* 0.007, MeOH)), while the mixture of **11** and **12** displayed significant optical activity ($[\alpha]_D +107.33^\circ$ (*c* 0.0006, MeOH)). This provides evidence that these bromomethoxy acetals are not artifacts of oxidation during the isolation process but are likely products of an enzymatic oxidation.

The isolation of tri-, tetra-, penta- and hexabrominated pyrrole alkaloids from *T. brasiliensis* is noteworthy. Prior to the present investigation, the 3,4,5-tribromo-1*H*-pyrrole-2-carboxylic acid was the only alkaloid presenting a tri-bromo acylpyrrole isolated from a marine sponge, *Axinella* sp.³¹ Because several bromine-substituted pyrroles have been isolated from cultures of marine bacteria,^{32,33} it is possible that sponge polybrominated pyrrole alkaloids may have a bacterial origin. However, recent investigations have shown that vanadium-dependent bromoperoxidases isolated from marine algae promote bromination of a variety of pyrrole derivatives,^{34–36} including that of 1*H*-pyrrole-2-carboxamide and 1*H*-pyrrole-2-carboxylate esters, which are commonly found in Agelasida and other marine sponges. Therefore, the distribution of brominated pyrroles in nature may not only be related to the diversity of bacteria associated with macroorganisms but possibly also to a widespread occurrence of bromoperoxidases in phylogenetically distant taxa. A recent metagenomic analysis of *Tedania brasiliensis* and other sponges presenting bromopyrrole alkaloids indicate that the biosynthesis of these compounds are related to the less abundant microbes in these sponges.³⁷

Derivatization of pseudoceratidine and synthesis of pseudoceratidine derivatives

Aiming to evaluate structure-activity relationships of pseudoceratidine and congeners in anti-parasitic assays, a series of 23 pseudoceratidine derivatives were synthesized. Natural pseudoceratidine was acetylated with Ac₂O in pyridine to obtain its *N*¹²-acetyl derivative (**2**). After HPLC purification of the acetylated product, we obtained both *N*¹²-acetyl pseudoceratidine (**2**) and *N*¹²-formyl pseudoceratidine (**3**). Compound **3** is likely derived from reaction of pseudoceratidine with acetic formic anhydride resulting from the reaction of Ac₂O and residual formic acid from the HPLC solvent used to purify pseudoceratidine. Compounds **2** and **3** were fully characterized by HRMS, ¹H, ¹³C, HSQC and HMBC spectra (Supporting Information).

In order to prepare additional pseudoceratidine derivatives in sufficient amounts for testing in several antiparasitic assays, the natural product was first synthesized based on a previously reported procedure.^{10,11} Commercially available 2,2,2-trichloro-1-(1*H*-pyrrol-2-yl)ethenone (**13**) was brominated with Br₂ to give the known di-brominated pyrrole (**14**)³⁸ in 87% yield. Coupling of **14** with spermidine (**15**) in THF provided synthetic pseudoceratidine in 72% yield (Scheme 1). *N*-Methyl-pseudoceratidine (**16**) was then prepared by reductive amination with formaldehyde in 70% yield to probe the importance of the basic secondary amine as a proton donor or acceptor, or both. Toward a derivative (**17**) amenable to further coupling with a fluorophore via Sharpless-Huisgen cycloaddition, pseudoceratidine (**1**) was coupled to 2-azidoacetic acid in 72% yield (Scheme 1).

A series of derivatives with different chains between the two pyrrole moieties were also synthesized to probe the importance of the chain length and the requirement of basic amines (Scheme 1). Compounds **20** and **21** were prepared using the same conditions for preparation of **1** employing 1,5-diaminopentane or 1,8-diaminooctane, in 50% and 74% yield from **14**, respectively. Pseudoceratidine derivatives **23** and **25** were prepared using similar conditions with spermine (**22**) and *N*¹-(6-aminohexyl)hexane-1,6-diamine (**23**), in 60% and 68% yield respectively. An additional variation introduced into the polyamine chain was introduction of a sulfur atom into the chain through synthesis of dialkyl sulfide **27** from 2-(2-aminoethylthio)ethanamine (**26**) and ketone **14** in a microwave reactor in 38% yield.

We also investigated changes in substituents on the pyrrole moieties while keeping the spermidine linker unchanged, with the exception of a non-brominated derivative of **20**, namely **28**, prepared in 60% yield by coupling of pyrrole ketone **13** and 1,5-diaminopentane (**18**). The spermidine derived non-brominated variant **29** was obtained in a similar manner in 70% yield. Monobromination of **13** at C-4 to provide **30** in 44% yield was achieved with 1-chloromethyl-4-fluor-1,4-diazoniabicyclo[2.2.2]octane bis(tetrafluoroborate) (Selectfluor or F-TEDA-BF₄) in the presence of KBr.³⁹ Reaction of **30** with spermidine (**15**) under the same conditions for the synthesis of pseudoceratidine gave 2,21-debromopseudoceratidine (**31**) in 65% yield. Chlorination of **13** with sulfuryl chloride provided 2,2,2-trichloro-1-(4,5-dichloro-1*H*-pyrrol-2-yl)ethenone (**32**) in 15% yield. Coupling of **32** with spermidine led to the chlorinated version of pseudoceratidine (**33**) in 38% yield. Monofluorination at C-5 of **13** was achieved with Selectfluor in a microwave reactor at 70 °C to provide **34** in 20% yield.⁴⁰ Coupling of **34** with spermidine under basic conditions gave **35** in 65% yield.

More substantial changes in the aromatic moieties of pseudoceratidine were also introduced. Coupling of indol-2-carboxylic acid (**36**) and 1*H*-benzo[*d*]imidazole-2-carboxylic acid (**37**) with spermidine gave derivatives **38** and **39** in moderate yields. Coupling with 5-bromothiophene-2-carboxylic acid (**40**) and 5-methylthiophene-2-carboxylic acid (**41**) gave **42** and **43** in low yield. Reaction of 6-chloropyridine-2-carboxylic acid (**44**) or 6-methylpyridine-2-carboxylic acid (**45**) with spermidine provided the pyridine derivatives **46** and **47** also in low yield. Finally, the coupling of furan derivatives **48** and **49** with spermidine enabled us to obtain bis-furans **50** and **51** in moderate yields.

Anti-parasitic Activity and SAR Investigation of Pseudoceratidine and Derivatives

Pseudoceratidine (**1**) was assayed against four protozoan parasite species: *P. falciparum*, *Leishmania (L.) amazonensis* (etiologic agent of localized and diffuse cutaneous leishmaniasis in South America), *L. (L.) infantum* (causative agent of visceral leishmaniasis in the Mediterranean and in Latin America) and *Trypanosoma cruzi*. Although **1** was essentially inactive against *L. (L.) amazonensis*, *L. (L.) infantum* and *T. cruzi*, it showed very good antiplasmodial activity ($1.1 \pm 0.1 \mu\text{M}$) against *P. falciparum* (Table 5). The inseparable mixture of structural isomers 3-debromopseudoceratidine (**4**) and 20-debromopseudoceratidine (**5**) showed five-fold decreased anti-parasitic activity on *P. falciparum* ($5.8 \pm 0.5 \mu\text{M}$), while *N*-acetyl-pseudoceratidine (**2**) did not display any anti-parasitic activity. The isomeric pair of tedamides A (**9**) and B (**10**) was also inactive as anti-parasitic agents. The preparation of pseudoceratidine derivatives **2**, **16**, **17**, **20**, **21**, **23**, **25**, **27** – **29**, **31**, **33**, **35**, **38**, **39**, **42**, **43**, **46**, **47**, **50** and **51** in adequate amounts enabled us to explore the impact on bioactivity through variation of the pseudoceratidine polyamine chain and aromatic end groups. *N*-Methyl-pseudoceratidine (**16**) showed good anti-plasmodial activity against *P. falciparum* ($4 \pm 1 \mu\text{M}$). Compound **23**, with a larger polyamine chain bearing two basic nitrogens, showed anti-plasmodial activity similar to that of the natural product ($1.9 \pm 1.2 \mu\text{M}$), while compound **25**, with a polyamine chain of similar length but with only one basic nitrogen, displayed a two-fold decrease in anti-plasmodial activity ($2 \pm 1 \mu\text{M}$). The 2,21-debromopseudoceratidine (**31**) derivative showed a decrease in anti-plasmodial activity ($7 \pm 1 \mu\text{M}$) relative to the pseudoceratidine (**1**). Finally, the furan derivative **51** bearing four bromine atoms also showed good anti-plasmodial activity against *P. falciparum* ($3 \pm 1 \mu\text{M}$).

Although pseudoceratidine (**1**) was inactive against *L. (L.) infantum* promastigotes, derivatives **20**, **23**, **27**, **42** and **50** showed enhanced, but yet moderate and similar, antileishmanial activity ($\text{EC}_{50\text{s}} \sim 20 \mu\text{M}$). The same derivatives were active, but considerably less potent, against *L. (L.) amazonensis*. Only compound **20** showed good anti-parasitic activity against *T. cruzi* epimastigotes, while compound **27** showed weak activity in the same bioassay.

Leishmania and *Trypanosoma* species are Euglenozoa kinetoplastida parasites, while *Plasmodium falciparum* belongs to Haemosporida within the phylum Apicomplexa.⁴¹ Constituting two groups of phylogenetically distant parasites, not surprisingly compounds affecting these two groups of organisms may show distinct effects. Our results indicated a selective, more potent activity, against *P. falciparum* for compounds **1**, **4** and **5**, **16**, **23**, **25**, **31** and **50** (Table 5 and Figure 2). It is evident the importance of bromine substituents in the aromatic extremities of pseudoceratidine derivatives for the anti-plasmodial activity. Fully debrominated pseudoceratidine (**29**) is completely inactive, as well as the chlorinated derivative **33** and fluorinated **35**. Although methyl groups represent a structural variation similar to bromine groups in terms of van der Waals radii,⁴² the bis-methylated bis-furan pseudoceratidine derivative **51** is completely inactive as well. Thus, bromination in both pyrrole and furan pseudoceratidine derivatives is essential for the expression of anti-plasmodial activity against *P. falciparum*, which seems to be related to the electronic effect of bromine on aromatic rings rather than to its van der Waals radius or to an enhanced lipophilic character promoted by the bromine substituents.⁴³ The nature of the polyamine

chain is an additional structural characteristic which determines the anti-plasmodial activity of pseudoceratidine derivatives. Compounds **20** and **21** which are devoid of a basic nitrogen, but have similar chain length (e.g., **21**) when compared to **1**, are inactive as anti-plasmodial agents. The sulfur bearing derivative **27** is inactive as well. On the other hand, compounds **23** and **25**, with longer polyamine chains, are as active as pseudoceratidine (**1**). The *N*-methyl derivative (**16**) is still active, but approximately four-fold less active than pseudoceratidine. Therefore, a basic linker in the form of the polyamine chain appears important for anti-plasmodial activity.

Derivatives with an *N*-acyl group (**2** and **17**) are inactive against *P. falciparum*, suggesting the importance of the basic nitrogens in the polyamine chain. These compounds were also inactive against *Leishmania* species and *T. cruzi* tested in our assays, which prevents simple acylation of pseudoceratidine to access cellular probes. However, alkylation of pseudoceratidine derivatives, was tolerated since they maintain the basic nitrogen atom. The selectivity index of the anti-plasmodial activity of compounds **1**, **4**, **5**, **16**, **23**, **25**, **31** and **50** was determined by measuring cytotoxicity on the human liver cancer HepG2 cell line (Table 5). Pseudoceratidine (**1**) was the most cytotoxic compound ($16 \pm 1 \mu\text{M}$), but with a selectivity index of 15. Compounds **16**, **4**, **5**, **23**, **25**, **31** and **50** displayed overall weak cytotoxicity, with selectivity indices between 35–125, which are considered excellent as this shows dramatically reduced toxicity to healthy cells.

As for the anti-Leishmanial activity, compounds **20**, **23**, **27**, **42** and **50** are moderate to weakly active (EC_{50} in the range between 19 and 24 μM ; Figure 3). However, a clear picture on the structural requirements for anti-Leishmanial activity of these pseudoceratidine derivatives did not emerge. Compounds **20** and **27** have shorter polyamine chains devoid of a basic nitrogen, but the opposite is true for compounds **23**, **42** and **50**. Bromination seems to be important, but the nature of the aromatic ring is apparently less relevant for the anti-leishmanial activity. Therefore, further variations on this series of anti-leishmanial compounds need to be explored in order to clarify structure-activity relationships aiming to improve the effectiveness of toxicity toward *Leishmania (L.) infantum* promastigotes.

In vitro infections were performed aiming to evaluate the activity of compounds **23**, **42** and **50** against *Leishmania* intracellular amastigotes. Because amastigotes must reside inside macrophages, we first determined the cytotoxicity of active pseudoceratidine derivatives against bone marrow derived macrophages from BALB/c mice. Compounds **23** and **42** showed low toxicity ($\text{CC}_{50} > 100 \mu\text{M}$). The half maximal cytotoxic concentration for compound **50** was $83 \pm 4 \mu\text{M}$. Compounds **23**, **42** and **50** were selected for further investigation of their activities on intracellular amastigotes. Bone marrow derived macrophages were infected with *L. (L.) amazonensis* stationary phase promastigotes ($\text{MOI} = 10$) for 24 h and then incubated with increasing concentrations of compounds **23**, **42** and **50** for subsequent counting of intracellular amastigotes. Intracellular parasitism was reduced in a dose-dependent manner after 24 h for **23**, **42** and **50** (Figure 4), leading to approximately 80% reduction of the amastigote number over the control group at higher concentrations. The intracellular effect against *Leishmania* amastigotes was almost equivalent when comparing compounds **23**, **42** and **50**. Further studies should evaluate the effects of compounds **23**, **42** and **50** in experimental leishmaniasis.

In order to better characterize the anti-plasmodial activity of pseudoceratidine (**1**), the most active compound against *P. falciparum*, its impact on the morphology of HepG2 cells was evaluated after 24 h of parasites treatment at a concentration 10-fold higher than its IC₅₀ value on the parasites. Pseudoceratidine (**1**) was not toxic for HepG2 cells at this high concentration as HepG2 cells showed microscopic morphology similar to untreated cells. Pseudoceratidine (**1**) was then tested against multi-resistant *P. falciparum* strain (K1 strain), and still presented very good potency against this K1 resistant strain, with an IC₅₀ value of $1.1 \pm 0.1 \mu\text{M}$ (Figure 5 and Table 6).

Aiming to assess the stage-specific inhibitory activity of pseudoceratidine (**1**), it was incubated at a concentration 10-fold higher than IC₅₀ values with highly-synchronized parasites. Cell morphological changes were observed by microscopy at 0 h, 8 h, 16 h and 32 h post-synchronization (Figure 6). Pseudoceratidine (**1**) showed inhibitory activity in the early ring stages, inducing alterations in *P. falciparum* morphology between 8 h and 16 h after incubation. These data suggest a fast-acting mechanism in which young forms of *P. falciparum* in the intraerythrocytic cycle are highly susceptible to the anti-parasitic activity of **1**. The potential drug interactions of pseudoceratidine (**1**) with sodium artesunate against *P. falciparum* were also assayed, in order to elucidate potential benefits and limitations of candidate molecules in combination with antimalarial drugs.⁴⁴ The isobologram analysis and FIC index (1.0 ± 0.2) indicate an additive interaction effect of pseudoceratidine (**1**) in combination with artesunate, thereby suggesting that pseudoceratidine derivatives may be used in artemisinin-based combination therapies (ACTs) (Figure 7).

Bromopyrrole alkaloids related to oroidin have been assayed against a series of parasites. Dispacamide B, spongiacidin B and dibromopalau'amine displayed anti-plasmodial activity against *P. falciparum* comparable to that of pseudoceratidine (1.34, 1.09 and 1.48 mg/mL, respectively).⁴⁵ Dibromopalau'amine was also very active against *T. brucei rhodesiense* (0.46 $\mu\text{g/mL}$) and against *Leishmania donovani* (1.48 $\mu\text{g/mL}$). Longamide B also showed good anti-parasitic activity against *T. brucei rhodesiense* (1.53 $\mu\text{g/mL}$) and against *L. donovani* (3.85 $\mu\text{g/mL}$).⁴⁵ Oroidin showed good anti-parasitic activity against *P. falciparum* (3.9 $\mu\text{g/mL}$) and moderate activity against *T. brucei rhodesiense* (17.3 $\mu\text{g/mL}$) being inactive against *Leishmania donovani* and *T. cruzi*.⁴⁶ Simpler derivatives 4,5-dibromo-1*H*-pyrrole-2-carboxylic acid and the respective methyl ester showed better anti-plasmodial activity (5.8 and 7.9 $\mu\text{g/mL}$, respectively).⁴⁶ It is clear that a detailed investigation of bromopyrrole alkaloids as anti-parasitic agents, particularly as anti-plasmodial compounds, is a worthy area for further research.

Conclusion

In the present investigation, we report the isolation of eight new pseudoceratidine derivatives from the sponge *Tedania brasiliensis*, of which the tedamides encompass a new 4-bromo-4-methoxy-5-oxo-4,5-dihydro-1*H*-pyrrole-2-carboxamide moiety. Pseudoceratidine displayed very good antimalarial activity, and justified the preparation of 23 of its derivatives aiming to establish initial structure-activity relationships. Pseudoceratidine and seven synthetic derivatives indicated that the length of the polyamine chain bearing a basic nitrogen, as well as the presence of bromine atoms on pyrrole or furan terminal moieties, represent essential

structural features for the expression of anti-plasmodial activity. Pseudoceratidine (**1**) showed antiplasmodial activity against both sensitive (3D7 strain) and resistant (K1 strain) *P. falciparum* strains, and also an additive interaction effect in combination with artesunate, indicating that derivatives of **1** may be used in combination with artemisinin for the treatment of malaria. The results described demonstrate that the pseudoceratidine scaffold, which is easily obtained by total synthesis, constitutes a useful lead to be developed as potential anti-plasmodial agents.

EXPERIMENTAL SECTION

General Experimental Procedures

UV spectra were recorded on a Shimadzu UV-3600 spectrophotometer. IR spectra were obtained on a Shimadzu IRAffinity-1 Fourier transform infrared spectrophotometer on a silica plate. NMR spectra were obtained at 25 °C, with TMS as an internal standard, using a Bruker ARX 9.4 Tesla spectrometer operating at either 400.35 MHz (¹H) or 100.10 MHz (¹³C) and a Bruker AV-600 spectrometer operating at either 600 MHz (¹H) or 150 MHz (¹³C) with a 2.5 mm cryoprobe. The ¹H chemical shifts are referenced to the residual DMSO-*d*₆ (δ2.49), whereas ¹³C chemical shifts are referenced to the DMSO-*d*₆ solvent peaks (δ39.5). HRMS and direct insertion MS/MS analyses were performed on a Waters Xevo QTOF MS/MS instrument using the following conditions: capillary voltage, 1.20 kV; desolvation temperature, 450 °C; voltage cone, 30 V; electrospray, positive mode; detection range, 100–1000 Da with total ion count extracting acquisition. Cone and desolvation gas flows were set to 700 L h⁻¹, respectively, with a nitrogen source. HPLC semi-preparative and preparative separations were performed with a Waters instrument (600 quaternary pump and 2487 double-beam UV detector), with 0.1% formic acid in all eluents utilized. HPLC-UV-ELSD-MS analyses were performed using a Waters Alliance 2695 instrument coupled on-line with a Waters 2996 photodiode array detector and a Waters 2424 evaporative light scattering detector, followed by a Micromass ZQ 2000 detector with an electrospray interface. The mass spectrometer detector was optimized using the following conditions: capillary voltage, 3.00 kV; source block temperature, 100 °C; desolvation temperature, 350°C; voltage cone, 25 V; electrospray, positive mode; detection range, 200–900 Da with total ion count extracting acquisition. Cone and desolvation gas flows were set to 50 and 350 L h⁻¹, respectively, with a nitrogen source.

Animal Material

The sponge *Tedania brasiliensis* was collected at Cabo Frio (Rio de Janeiro state, in April 2011) and identified by one of the authors (E.H.). A voucher of the collected sponge has been deposited at the Museu Nacional do Rio de Janeiro, Universidade Federal do Rio de Janeiro (MNRJ 16876).

Extraction and Isolation

A 136.2 g freeze-dried sample of *T. brasiliensis* was homogenized and exhaustively extracted with 5 L of MeOH. The solvent was evaporated to 500 mL. The resulting MeOH extract was diluted with 50 mL of H₂O and partitioned with hexane (3 × 500 mL). The MeOH/H₂O fraction was evaporated to dryness and dissolved in 1 L of 1:1 EtOAc/H₂O.

Partitioning was performed two additional times. The EtOAc fraction was evaporated to dryness to yield 5.37 g. The hexane extract was also evaporated to dryness to yield 1.79 g of an apolar fraction. The aqueous fraction of the EtOAc/H₂O partition was extracted with a 1:1 mixture of XAD-4 and XAD-7, after which the resins were desorbed with MeOH, then with 1:1 MeOH/acetone, and the organic solvents were evaporated to dryness. Anti-parasitic assays performed with the hexanes, EtOAc and resin-extracted H₂O fraction indicated bioactivity exclusively in the EtOAc fraction. HPLC-UV-MS analysis of these three fractions indicated pseudoceratidine (**1**) and its minor derivatives only in the EtOAc fraction as well. Therefore, neither the hexanes nor resin-extracted H₂O fractions were investigated.

The EtOAc fraction (5.37 g) was subjected to solid-phase extraction on a C₁₈ reversed-phase cartridge (Waters) eluted with a gradient of MeOH in H₂O. After their evaporation and TLC analysis, the fractions obtained were pooled into eight fractions named TBA1 (608 mg), TBA2 (567 mg), TBA3 (347 mg), TBA4 (377 mg), TBA5 (251 mg), TBA6 (383 mg), TBA7 (338 mg) and TBA8 (399 mg). Fraction TBA2 was separated by HPLC using an Inertsil ODS-2 column (250 × 9.4 mm, 5 μm), with a H₂O/MeCN ratio of 75:25, a flow rate of 1.5 mL/min and detection performed at λ_{max} 254 nm. Six fractions were obtained, among which fraction TBA2B (42.1 mg) was further investigated and fraction TBA2F (28.1 mg) was identified as 4,5-dibromo-1*H*-pyrrole-2-carboxylic acid. Fraction TBA2B was separated by HPLC using an Inertsil ODS-2 column (250 × 9.4 mm, 5 μm), with a H₂O/MeCN ratio of 67:33, a flow rate of 1.5 mL/min and detection performed at λ_{max} 254 nm. Seven fractions were obtained, among which fraction TBA2B3 (9.4 mg) was identified as a mixture of tedamides A (**9**) and B (**10**), fraction TBA2B5 (1.3 mg) was identified as 3-debromopseudoceratidine (**4**) and 20-debromopseudoceratidine (**5**) and fraction TBA2B7 (10.2 mg) was identified as pseudoceratidine (**1**).⁸

HPLC separation of the fraction TBA3 using an Inertsil ODS-2 column (250 × 9.4 mm, 5 μm), with a gradient of MeOH in H₂O from 40% MeOH to 100% MeOH over 45 min (flow rate of 1.5 mL/min and detection at λ_{max} 254 nm), yielded six fractions, among which fraction TBA3-4 (71.8 mg) was identified as pure pseudoceratidine (**1**) and fractions TBA3-3 (17.0 mg), TBA3-5 (13.3 mg) and TBA3-6 (4.3 mg) were further investigated. Fraction TBA3-3 was separated using an Inertsil ODS-3 column (250 × 4.6 mm, 5 μm), with a gradient of MeOH in H₂O from 38% MeOH to 60% MeOH over 38 min (flow rate of 1.0 mL/min and detection at λ_{max} 254 nm), to yield six fractions, among which TBA3-3C (2.3 mg) was identified as a mixture of tedamides C (**11**) and D (**12**). Fraction TBA3-5 (13.3 mg) was separated by HPLC using an Inertsil ODS-3 column (250 × 4.6 mm, 5 μm), with a gradient of MeOH in H₂O from 10% MeOH to 100% MeOH over 35 min (flow rate of 1.0 mL/min and detection at λ_{max} 254 nm), to yield four fractions, among which fraction TBA3-5B (2.7 mg) was further purified using an Inertsil ODS-3 column (250 × 4.6 mm, 5 μm), with a gradient of MeOH in H₂O from 55% MeOH to 60% MeOH over 30 min (flow rate of 1.0 mL/min and detection at λ_{max} 254 nm), to yield pure 19-bromopseudoceratidine (**7**) (1.0 mg). Fraction TBA3-6 (4.3 mg) was purified by HPLC using an Inertsil ODS-3 column (250 × 4.6 mm, 5 μm), with a gradient of MeOH in H₂O from 10% MeOH to 100% MeOH over 35 min (flow rate of 1.0 mL/min and detection at λ_{max} 254 nm), to yield 0.5 mg of 4,19-dibromopseudoceratidine (**8**).

Separation of fraction TBA-5 (250.5 mg) by HPLC using an Inertsil ODS-2 column (250 × 9.4 mm, 5 μm) and a gradient of 1:1 MeOH/MeCN in H₂O, from 44% to 100% of the organic mixture over 30 min, yielded seven fractions, among which TBA-5D (80.7 mg) was identified as pure pseudoceratidine (**1**).

Separation of the fraction TBA-7 (338 mg) by HPLC using an Inertsil ODS-2 column (250 × 9.4 mm, 5 μm), with a gradient of MeOH/MeCN (1:1) in H₂O from 44% MeOH to 100% MeOH/MeCN (1:1) over 35 min (flow rate of 1.5 mL/min and detection at λ_{max} 254 nm), yielded fraction TBA-7A (98.2 mg). This fraction was further separated by HPLC using an Inertsil ODS-3 column (250 × 4.6 mm, 5 μm), with a gradient of MeOH/MeCN (1:1) in H₂O from 30% to 100% MeOH/MeCN (1:1) over 30 min (flow rate of 1.0 mL/min and detection at λ_{max} 254 nm), to yield ten fractions, among which TBA-7A8 (5.0 mg) was identified as a mixture of 4-bromopseudoceratidine (**6**) and 19-debromopseudoceratidine (**7**).

3-Debromopseudoceratidine (**4**) and *20-debromopseudoceratidine* (**5**): colorless glassy solid; UV (MeOH) λ_{max} (log ε) 215 (4.2), 235 (4.2), 274 (4.6) nm; IR (film) ν_{max} 3186, 2945, 1677, 1629, 1133, 740, and 615 cm⁻¹; ¹H and ¹³C NMR data, Tables 1 and 2; HRESIMS: *m/z* 565.9409 [M+H]⁺ (calcd for C₁₇H₂₃⁷⁹Br₃N₅O₂, 565.9402).

4-Bromopseudoceratidine (**6**) and *19-bromopseudoceratidine* (**7**): colorless glassy solid; UV (MeOH) λ_{max} (log ε) 215 (4.2), 235 (4.2), 277 (4.6) nm; ¹H and ¹³C NMR data, Tables 1 and 2; HRESIMS: *m/z* 721.7632 [M+H]⁺ (calcd for C₁₇H₂₁⁷⁹Br₅N₅O₂, 721.7612).

4,19-Dibromopseudoceratidine (**8**): glassy solid; UV (MeOH) λ_{max} (log ε) 222 (4.2), 235 (4.2), 274 (4.6) nm; ¹H and ¹³C NMR data, Tables 1 and 2; HRESIMS: *m/z* 799.6749 [M+H]⁺ (calcd for C₁₇H₂₀⁷⁹Br₆N₅O₂, 799.6717).

Tedamide A (**9**) and *tedamide B* (**10**): colorless glassy solid; [α]_D -7.75° (*c* 0.007, MeOH); UV (MeOH) λ_{max} (log ε) 218 (4.2), 275 (4.2) nm; IR (film) ν_{max} 3103, 2938, 2842, 1718, 1677, 1526, 1202, 1139, and 719 cm⁻¹; ¹H and ¹³C NMR data, Tables 3 and 4; HRESIMS: *m/z* 611.9452 [M+H]⁺ (calcd for C₁₈H₂₅⁷⁹Br₃N₅O₄, 611.9456).

Tedamide C (**11**) and *tedamide D* (**12**): colorless glassy solid; [α]_D +107.33° (*c* 0.0006, MeOH); UV (MeOH) λ_{max} (log ε) 218 (4.2), 275 (4.2) nm; ¹H and ¹³C NMR data, Tables 3 and 4; HRESIMS: *m/z* 689.8571 [M+H]⁺ (calcd for C₁₈H₂₄⁷⁹Br₄N₅O₄, 689.8562).

Preparation of *N*¹²-Acetylpseudoceratidine (**2**) and *N*¹²-Formylpseudoceratidine (**3**)

Pseudoceratidine (**1**, 5.0 mg, 7.7 mM) was dissolved in freshly distilled pyridine (1 mL) and acetic anhydride (1 mL, 10.6 mM) was added. The reaction was left under magnetic stirring for 60 h, after which the pyridine/Ac₂O mixture was evaporated *in vacuo*. The reaction mixture was purified by HPLC using an Inertsil ODS-3 column (250 × 4.6 mm, 5 μm), with 65% MeOH, a flow rate of 1.0 mL/min and detection performed at λ_{max} 254 nm. *N*¹²-Acetylpseudoceratidine (**2**) (2.7 mg) and *N*¹²-formylpseudoceratidine (**3**) (1.4 mg) were obtained in 50.7% and 26.9% yields, respectively.

*N*¹²-Acetylpseudoceratidine (**2**): colorless glassy solid; UV (MeOH) λ_{max} (log ε) 222 (4.2), 235 (4.2), 275 (4.6) nm; IR (film) ν_{max} 2924, 2842, 1608, 1560, 1526, and 664 cm⁻¹; ¹H

and ^{13}C NMR data, Tables 1 and 2; HRESIMS: m/z 683.8433 $[\text{M}-\text{H}]^-$ (calcd for $\text{C}_{19}\text{H}_{22}^{79}\text{Br}_4\text{N}_5\text{O}_3$, 683.8456).

*N*¹²-Formylpseudoceratidine (**3**): colorless glassy solid; UV (MeOH) λ_{max} (log ϵ) 222 (4.2), 235 (4.2), 275 (4.6) nm; IR (film) ν_{max} 2924, 2842, 1587, 1360, and 650 cm^{-1} ; ^1H and ^{13}C NMR data, Tables 1 and 2; HRESIMS: m/z 669.8283 $[\text{M}-\text{H}]^-$ (calcd. for $\text{C}_{18}\text{H}_{22}^{79}\text{Br}_4\text{N}_5\text{O}_3$, 671.8299).

Bioassay procedures

Chemical Compounds—Alamar blue (resazurin), DMSO and MeOH, M-199 medium, RPMI-1640, phosphate-buffered saline (PBS), sodium azide (99.5% purity), bacterial lipopolysaccharide (99% purity) and TritonX-100 (99% purity), benznidazole (97% purity) were purchased from commercial suppliers.

Anti-Leishmanial and Anti-*Trypanosoma cruzi* in vitro Assays—*Leishmania (L.) amazonensis* (MHOM/BR/1973/M2269) promastigotes were maintained at 26 °C in Medium 199 (Sigma-Aldrich) supplemented with 5% penicillin/streptomycin, 0.1% hemin (25 mg/mL in 50% triethanolamine), 20% heat-inactivated fetal bovine serum (FBS), 10 mM adenine (pH 7.5), and 5 mM L-glutamine.⁴⁷ *Leishmania (L.) infantum* (MHOM/BR/1972/LD) was cultured as described above, with the exception that 5% human sterile urine was added to the culture medium. *Trypanosoma cruzi* epimastigotes (Y strain) were grown in liver infusion tryptose (LIT) medium supplemented with 20 mg/L hemin and 10% fetal calf serum at 28 °C as previously described.⁴⁸ The anti-parasitic activity of pseudoceratidine derivatives was assessed against trypanosomatids, using a MTT viability assay⁴⁹ after 24 h incubation with the series of pseudoceratidine derivatives. The half maximal effective concentration (EC₅₀) values for the *Leishmania* spp. and *T. cruzi* populations were calculated from sigmoidal regression of the concentration-response curves using Scientific Graphing and Analysis Software Origin 5.0. Each experiment was performed in triplicate and repeated two or three times. Cytotoxic experiments were conducted using bone marrow macrophages from BALB/c female mice. Differentiated cells were cultured in 96 well plates at 37 °C for posterior incubation with increasing concentrations of pseudoceratidine derivatives for 24 h. The MTT method was also performed and CC₅₀ values were calculated accordingly.⁴⁹

Intracellular infections were obtained by infecting bone marrow derived macrophages with stationary phase *L. (L.) amazonensis* promastigotes (10 parasites: 1 macrophage; MOI = 10). After 1 h of incubation with the parasites, cultures were washed three times with PBS 1X and maintained at 33 °C, 5% CO₂, for 24 h. After this period, infections were established and different concentrations of pseudoceratidine compounds were added to the cultures that remained at 33 °C for 24 h. Cells were then washed three times with warm PBS 1X and fixed with MeOH for subsequent staining using Instant Prov kit (Newprov). The number of intracellular amastigotes was obtained by counting 300 cells in triplicate coverslips. Photomicrographs of infections were recorded using the microscope system *Leica* LAS Core. Experiments using BALB/c mice were approved by the Ethical Committee for Animal

Experimentation of the Biology Institute of the State University of Campinas – UNICAMP (4535-1/2017).

Anti-Plasmodial in vitro Assays Against *P. falciparum* Blood Parasites—

Plasmodium falciparum blood parasites [3D7, sensitive strain; K1, chloroquine, cycloguanil and pyrimethamine resistant strain] were cultured as previously described.⁵⁰ Freshly sorbitol synchronized ring stages⁵¹ were incubated with the test samples at various concentrations, previously solubilized in 0.05% DMSO (v/v). Each assay was performed in triplicate. Results were compared with control cultures in complete medium with no assay samples. Pyrimethamine, chloroquine, cycloguanil and sodium artesunate were used in each experiment as antimalarial controls. The activity of test samples was measured using the SYBR green assay.⁵² Briefly, the plates were centrifuged at 700g for 5 min at room temperature to remove the medium, washed with 1X PBS and incubated for 30 min with lysis buffer solution [2.4228 g TRIS, ultra-pure (for 20 mM solution), pH 7.5; 1.8612 g of EDTA 5 mM ultrapure (for 5 mM solution); 80 µg saponin (0.008% w/v); 800 µL of Triton X-100 (0.08% v/v); H₂O Type I] and SYBR green I DNA stain (1: 20000). The fluorescence of uninfected erythrocytes was considered as a background. Fluorescence was measured on a SpectraMax340PC384 fluorimeter at 485/535 nm. The half-maximal compound inhibitory concentration (IC₅₀) was estimated by curve fitting using software from the OriginLab Corporation and comparing to the parasite growth in test sample-free medium.

Cytotoxicity Tests Using Immortalized Cells—The cytotoxicity of test compounds was evaluated in a human hepatoma cell line (HepG2) using cells cultured in 75 cm² sterile flasks containing RPMI-1640 medium (supplemented with 10% heat-inactivated fetal bovine serum and 40 mg/L gentamicin) under a 5% CO₂ atmosphere at 37 °C. When confluent, the cell monolayer was washed with culture medium, trypsinized, distributed in a flat-bottomed 96-well plate (5 × 10³ cells/well) and incubated for 18 h at 37 °C for cell adherence.⁵³ The compounds (in 20 µL solution) at various concentrations (1,000-1 µg/mL) were placed in 96-well plates and incubated with the cultured cells for 24 h under a 5% CO₂ atmosphere at 37 °C. Then, 3-(4,5-dimethylthiazol-2-yl)-2,5-diphenyltetrazolium bromide (MTT) solution (5 mg/mL; 20 µL/well for 3 h) was used to evaluate the mitochondrial viability. The supernatants were carefully removed and 100 µL DMSO was added to each well and mixed to solubilize the formazan crystals. The optical density was determined at 570 nm and 630 nm. The cell viability was expressed as the percentage of the control absorbance in the untreated cells after subtracting the appropriate background.

In vitro Association with Artesunate—The isobologram was built to analyze the effects of drug combination aiming to determining the additive, synergic or antagonistic effect. Briefly, the fractional half maximum inhibitory concentration (FIC₅₀) was calculated for each drug pair combination. A stock drug solution was prepared for each drug using complete media, such that the final concentration approximates IC₅₀ following 3–4 twofold dilutions. Using these stocks solutions, the following volume-volume (v/v) mixtures of artesunate and pseudoceratidine (**1**) were prepared in 0:5, 1:4, 2:3, 1:4 and 5:0 ratios. These mixtures were two-fold serially diluted to generate a range of seven concentrations in each case. The ΣFIC₅₀ were calculated using the equation: FIC₅₀ artesunate (IC₅₀ of artesunate

when combined with pseudoceratidine/artesunate IC_{50}) + FIC_{50} pseudoceratidine (IC_{50} of pseudoceratidine when combined with artesunate/pseudoceratidine IC_{50}). Isobologram curves were constructed by plotting FIC_{50} , pseudoceratidine vs FIC_{50} , artesunate. A straight diagonal line ($\Sigma FIC_{50} = 1$) indicates an additive effect between artesunate and pseudoceratidine, a concave curve below the diagonal ($FIC_{index} < 1$) indicates a synergistic effect and a convex curve above the diagonal ($FIC_{index} > 1$) indicates antagonism.⁵⁴

Supplementary Material

Refer to Web version on PubMed Central for supplementary material.

Acknowledgments

The authors thank Dr. Haoran Xue (Baylor University) for help in the characterization of some of the synthetic derivatives and Dr. D. E. Williams (Department of Earth, Ocean and Atmospheric Sciences, University of British Columbia), for his assistance in some of the HRMS measurements. Financial support was provided by a FAPESP BIOTA/BIOprospecTA grant (2013/50228-8) awarded to RGSB, CEPID-CIBFar grant (2013/07600-3) to GO, CNPq (grants 471509/2012-4 and 405330/2016-2) to RVCG, FAPESP Young Investigators Grant (2014/21129-4) to DCM and a FAPESP Regular Research Grant (2015/24595-9) to FRG. LLLP and AFB thanks CAPES for a PhD scholarship, and also for a Science without Borders scholarship at Baylor University for AFB. D. R. acknowledges the financial support from NIH (R37 GM052964) and from the Robert A. Welch Foundation (AA-1280).

References

- Blunt JW, Copp BR, Keyzers RA, Munro MHG, Prinsep MR. *Nat Prod Rep.* 2017; 34:235–294. and previous reviews in this series. [PubMed: 28290569]
- Wang X, Ma Z, Wang X, De S, Ma Y, Chen C. *Chem Commun.* 2014; 50:8628–8639.
- Al-Mourabit A, Zancanella MA, Tilvic S, Romo D. *Nat Prod Rep.* 2011; 28:1229–1260. [PubMed: 21556392]
- Braekman JC, Daloz D, Stoller C, van Soest RWM. *Biochem Syst Ecol.* 1992; 20:417–431.
- van Soest RWM, Braekman JC. *Mem Queensland Mus.* 1999; 44:569–589.
- Erpenbeck D, van Soest RWM. *Mar Biotechnol.* 2007; 9:2–19. [PubMed: 16817029]
- Cárdenas P, Pérez T, Boury-Esnault N. *Adv Mar Biol.* 2012; 61:79–209. [PubMed: 22560778]
- Tsukamoto S, Kato H, Hirota H, Fusetani N. *Tetrahedron Lett.* 1996; 37:1439–1440.
- Tsukamoto S, Kato H, Hirota H, Fusetani N. *Tetrahedron.* 1996; 52:8181–8186.
- Ponasiak JA, Kassab DJ, Ganem B. *Tetrahedron Lett.* 1996; 37:6041–6044.
- Behrens C, Christoffersen MW, Gram L, Nielsen PH. *Bioorg Med Chem Lett.* 1997; 7:321–326.
- Ariey F, Witkowski B, Amaratunga C, Beghain J, Langlois AC, Khim N, Kim S, Duru V, Bouchier C, Ma L, Lim P, Leang R, Duong S, Sreng S, Suon S, Chuor CM, Bout DM, Ménard S, Rogers WO, Genton B, Fandeur T, Miotto O, Ringwald P, Le Bras J, Berry A, Barale JC, Fairhurst RM, Benoit-Vical F, Mercereau-Puijalon O, Ménard D. *Nature.* 2014; 505:50–55. [PubMed: 24352242]
- World Health Organization; 2016. www.who.int/leishmaniasis/en/ [Accessed in August, 2107]
- Kedzierski L, Sakthianandeswaren A, Curtis JM, Andrews PC, Junk PC, Kedzierska K. *Curr Med Chem.* 2009; 16:599–614. [PubMed: 19199925]
- Croft SL, Olliaro P. *Clin Microbiol Infect.* 2011; 17:1478–83. [PubMed: 21933306]
- Tempone AG, Sartorelli P, Mady C, Fernandes F. *Cardiovasc Hematol Agents Med Chem.* 2007; 5:222–235. [PubMed: 17630949]
- Gascon J, Bern C, Pinazo MJ. *Acta Trop.* 2010; 115:22–27. [PubMed: 19646412]
- Schmunis GA, Yadon ZE. *Acta Trop.* 2010; 115:14–21. [PubMed: 19932071]
- Globalization and infectious diseases, a review of the linkages. *WHO Special Topics.* 2013; 3
- Pereira PC, Navarro ECJ. *Venom Anim Toxins Incl Trop Dis.* 2013; 19:19–34.

21. Santos MFC, Harper PM, Williams DE, Mesquita JT, Pinto EG, Costa-Silva TA, Hajdu E, Ferreira AG, Santos RA, Murphy PJ, Andersen RJ, Tempone AG, Berlinck RGS. *J Nat Prod.* 2015; 78:1101–1112. [PubMed: 25924111]
22. Reimão JQ, Migotto AE, Kossuga MH, Berlinck RGS, Tempone AG. *Parasitol Res.* 2008; 103:1445–1450. [PubMed: 18762984]
23. Kossuga MH, Nascimento AM, Reimão JQ, Tempone AG, Taniwaki NN, Veloso K, Ferreira AG, Cavalcanti BC, Pessoa C, Moraes MO, Mayer AMS, Hajdu E, Berlinck RGS. *J Nat Prod.* 2008; 71:334–339. [PubMed: 18177008]
24. Gray CA, de Lira SP, Silva M, Pimenta EF, Thiemann OH, Oliva G, Hajdu E, Andersen RJ, Berlinck RGS. *J Org Chem.* 2006; 71:8685–8690. [PubMed: 17080994]
25. Somsák L, Kovács L, Tóth M, Ösz E, Szilágyi L, Györgydeák Z, Dinya Z, Docsa T, Tóth B, Gergely PJ. *Med Chem.* 2001; 44:2843–2848.
26. Czifrák K, Somsák L. *Tetrahedron Lett.* 2002; 43:8849–8852.
27. Czifrák K, Szilágyi P, Somsák L. *Tetrahedron Asym.* 2005; 16:127–141.
28. Czifrák K, Gyóllai V, Kövér KE, Somsák L. *Carbohydr Res.* 2011; 346:2104–2112.
29. Hanington PM, Jung ME. *Tetrahedron Lett.* 1994; 35:5145–5148.
30. Somsák L, Nagy V. *Tetrahedron Asym.* 2000; 11:1719–1727.
31. Barrow RA, Capon R. *J Nat Prod Lett.* 1993; 1:243–250.
32. Gribble GW. *Fortschr Chem Org Naturst.* 2010; 91:1–505. [PubMed: 19953383]
33. Andersen RJ, Wolfe MS, Faulkner DJ. *Mar Biol.* 1974; 27:281–285.
34. Wischang D, Hartung J. *Tetrahedron.* 2011; 67:4048–4054.
35. Wischang D, Radlow M, Schulz H, Vilter H, Viehweger L, Altmeyer MO, Kegler C, Herrmann J, Müller R, Gaillard F, Delage L, Leblanc C, Hartung J. *J Bioorg Chem.* 2012; 44:25–34.
36. Wischang D, Radlow M, Hartung J. *Dalton Trans.* 2013; 42:11926–11940. [PubMed: 23881071]
37. Rua CPJ, Oliveira L, Froes A, Tschoeke DA, Soares AC, Leomil L, Gregoracci GB, Hajdu E, Thompson CC, Berlinck RGS, Thompson FL. 2017 submitted.
38. Bailey DM, Johnson RE. *J Med Chem.* 1973; 16:1300–1302. [PubMed: 4201185]
39. Ye C, Shreeve JM. *J Org Chem.* 2004; 24:8561–8563.
40. Troegel B, Lindel T. *Org Lett.* 2012; 14:468–471. [PubMed: 22191556]
41. Berman, JJ. *Taxonomic Guide to Infectious Diseases: Understanding the Biologic Classes of Pathogenic Organisms.* Academic Press; Amsterdam: 2012. p. 95-98.
42. Bazzini, P., Wermuth, CG. *The Practice of Medicinal Chemistry.* 4. Wermuth, CG, Aldous, D, Raboisson, P., Rognan, D., editors. Elsevier; Amsterdam, Boston: 2015. p. 338
43. Bazzini, P., Wermuth, CG. *The Practice of Medicinal Chemistry.* 4. Wermuth, CG, Aldous, D, Raboisson, P., Rognan, D., editors. Elsevier; Amsterdam, Boston: 2015. p. 341
44. Wells TN, Hooft van Huijsduijnen R, Van Voorhis WC. *Nat Rev Drug Discov.* 2015; 6:424–442.
45. Scala F, Fattorusso E, Menna M, Tagliatalata-Scafati O, Tierney M, Kaiser M, Tasdemir D. *Mar Drugs.* 2010; 8:2162–2174. [PubMed: 20714430]
46. Tasdemir D, Topaloglu B, Perozzo R, Brun R, O'Neill R, Carballeira NM, Zhang X, Tonge PJ, Linden A, Ruedi P. *Bioorg Med Chem.* 2007; 15:6834–6845. [PubMed: 17765547]
47. Miguel DC, Flannery AR, Mittra B, Andrews NW. *Infect Immun.* 2013; 81:3620–3626. [PubMed: 23876801]
48. Peloso EF, Dias L, Queiroz RM, Leme AF, Pereira CN, Carnielli CM, Werneck CC, Sousa MV, Ricart CA, Gadelha FR. *Biochim Biophys Acta.* 2016; 1:1–10.
49. Miguel DC, Yokoyama-Yasunaka JK, Andreoli WK, Mortara RA, Uliana SR. *J Antimicrob Chemother.* 2007; 3:526–34.
50. Trager W, Jensen JB. *Science.* 1976; 193:673–675. [PubMed: 781840]
51. Lambros C, Vanderberg JP. *J Parasitol.* 1979; 65:418–420. [PubMed: 383936]
52. Smilkstein M, Sriwilaijaroen N, Kelly JX, Wilairat P, Riscoe M. *Antimicrob Agents Chemother.* 2004; 48:1803–18063. [PubMed: 15105138]
53. Denizot F, Lang R. *J Immunol Methods.* 1986; 89:271–277. [PubMed: 3486233]

54. Gorka AP, Jacobs LM, Roepe PD. *Malar J.* 2013; 12:332. [PubMed: 24044530]

Author Manuscript

Author Manuscript

Author Manuscript

Author Manuscript

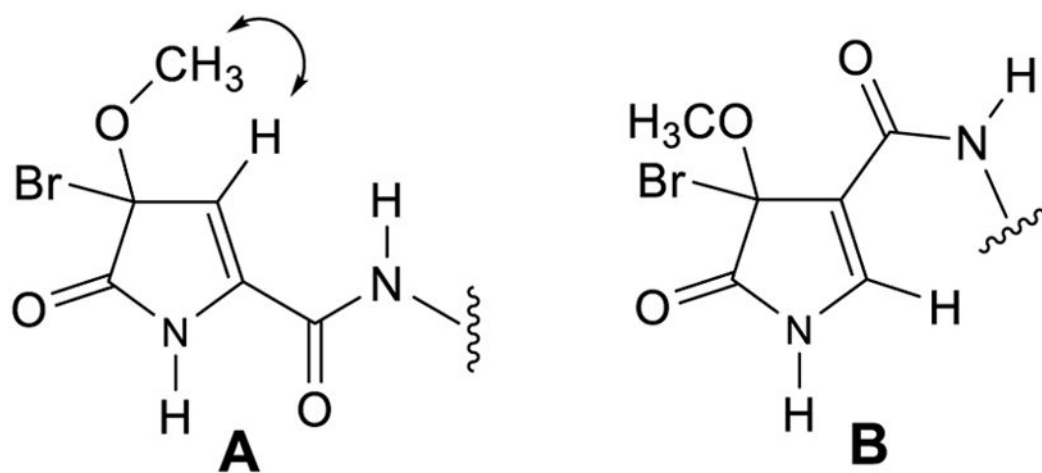


Figure 1. NOE observed in the 1D NOESY spectrum of tedamides A (**9**) and B (**10**) that supports the presence of fragment A instead of fragment B in the structures of **9** and **10**.

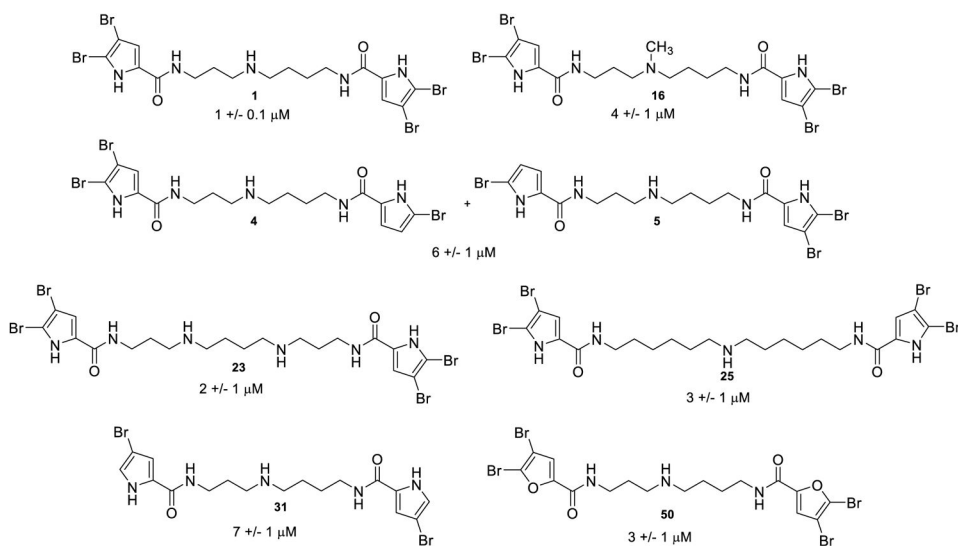


Figure 2. Structures and anti-plasmodial activities of pseudoceratidine derivatives against *Plasmodium falciparum*.

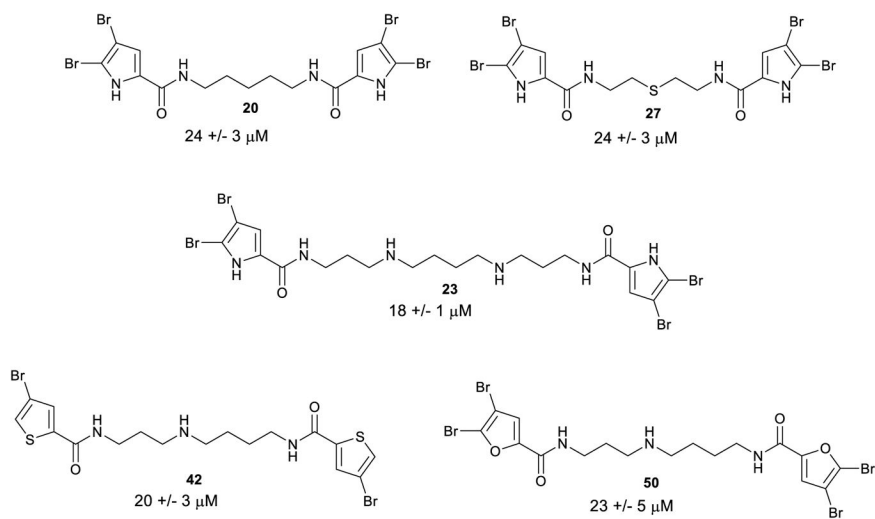


Figure 3. Structures and anti-leishmanial activities of pseudoceratidine derivatives against *Leishmania (L.) infantum*.

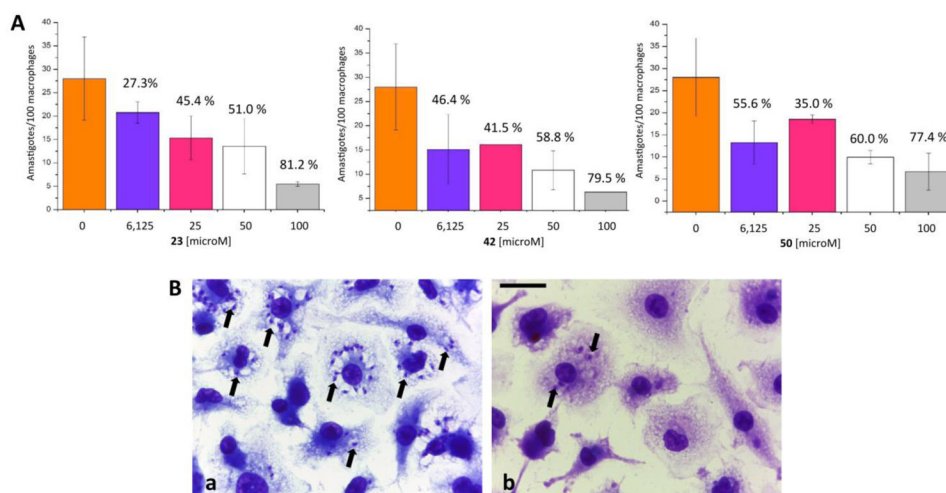


Figure 4. *In vitro* activity of **23**, **42** and **50** against intracellular *L. (L.) amazonensis* amastigotes. Macrophages derived from BALB/c mice bone marrow were infected with *L. (L.) amazonensis* stationary promastigotes for 1 h (MOI = 10). After 24 h, infected cells were incubated with 6.125, 25, 50 or 100 μM of each compound for 24 h. MeOH-fixed cells were stained and infection was determined by counting 300 cells/coverslip. Experiments were performed in triplicate. The results shown are representative of two independent experiments. A. Bars indicate the number of intracellular amastigotes. Numbers above each bar indicate the percentage of reduction over control untreated infected macrophages. (B) Photomicrograph examples showing untreated infected macrophages (a) and infected macrophages incubated with compound **42** at 100 μM (b). Arrows point to intracellular amastigotes. Bar = 10 μm.

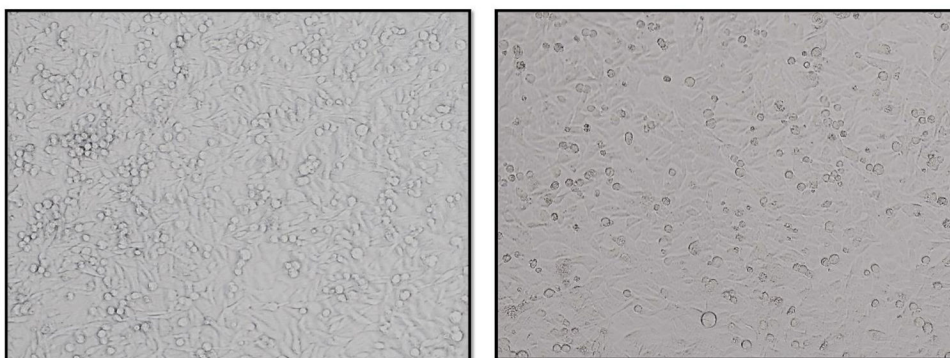


Figure 5. HepG2 cells morphology before (left) and after (right) treatment with pseudoceratinidina (**1**) at 10 μ M.

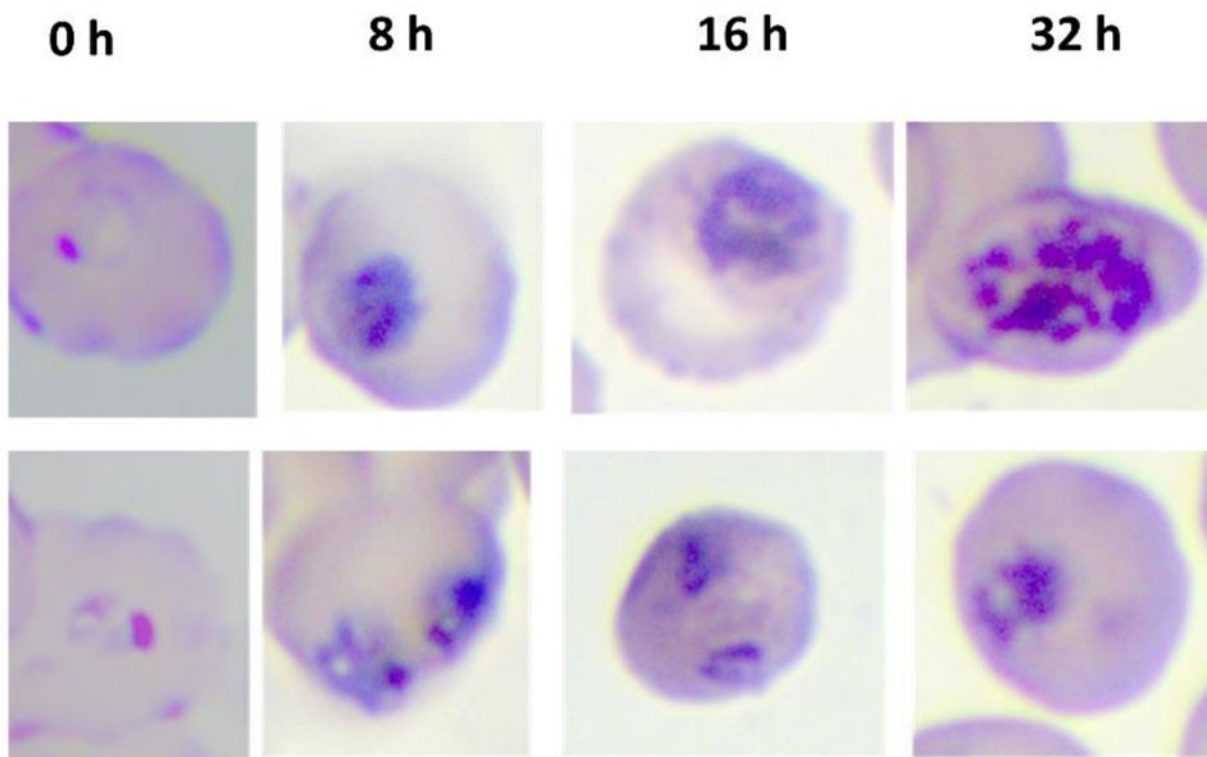


Figure 6. Microscopy of synchronized parasites continuously treated with pseudoceratidine (**1**) at concentration 10-fold the IC₅₀ value (top line) and DMSO (control, bottom line). Images are representative of three independent experiments.

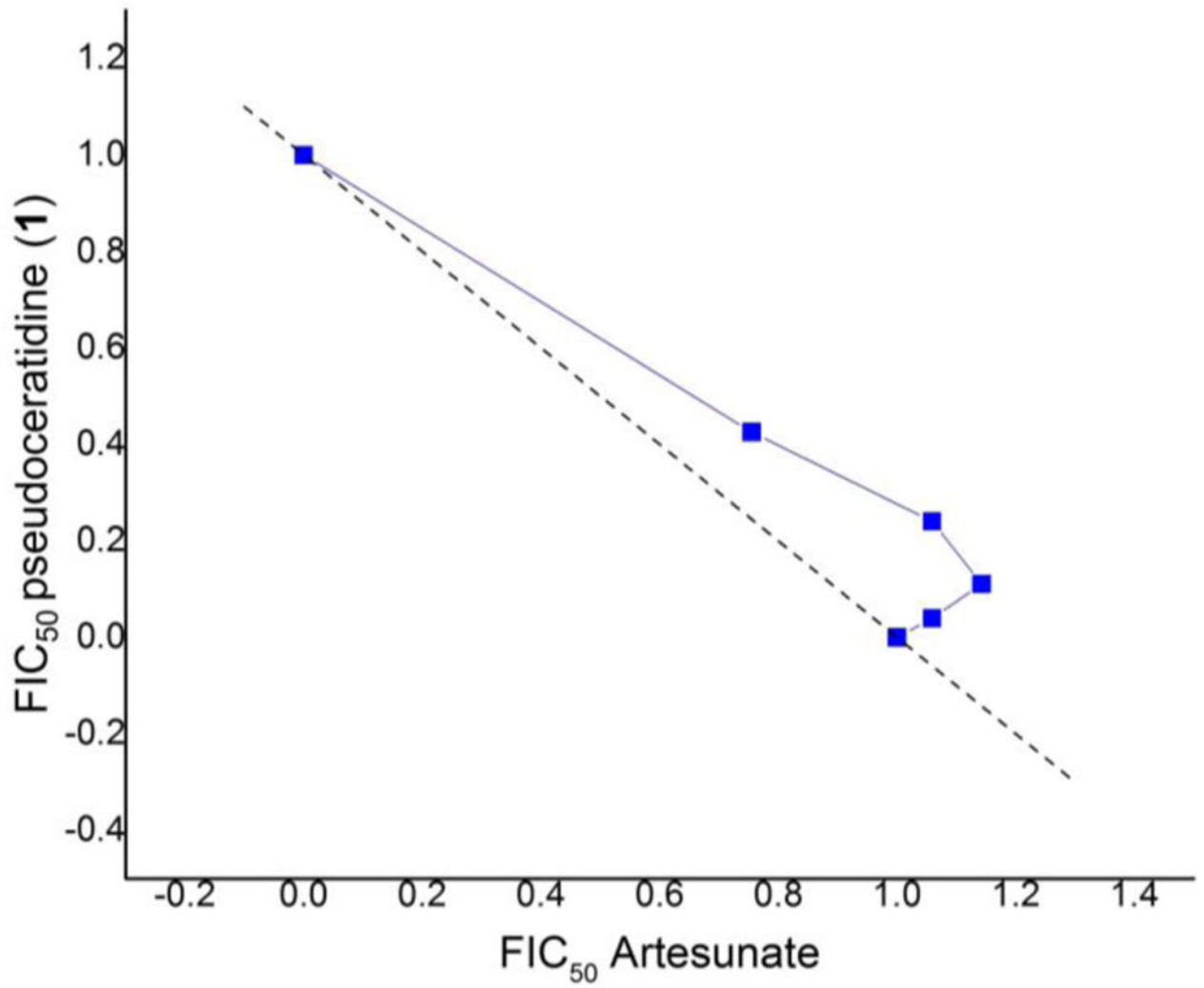
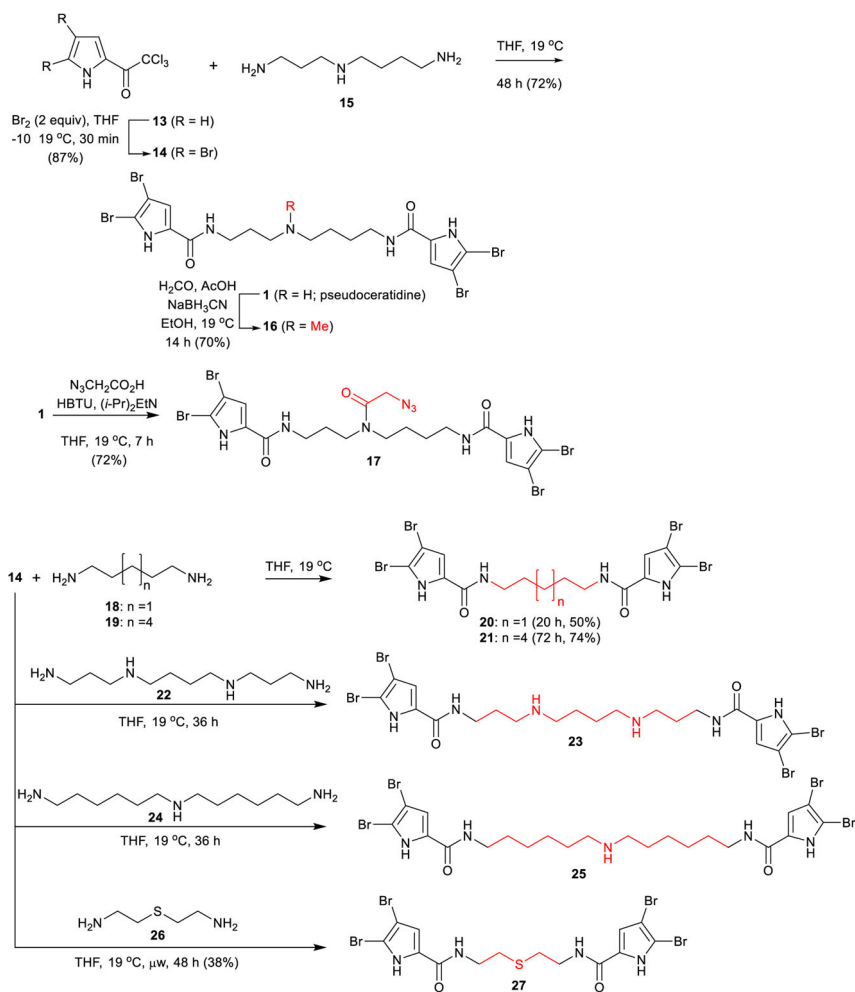
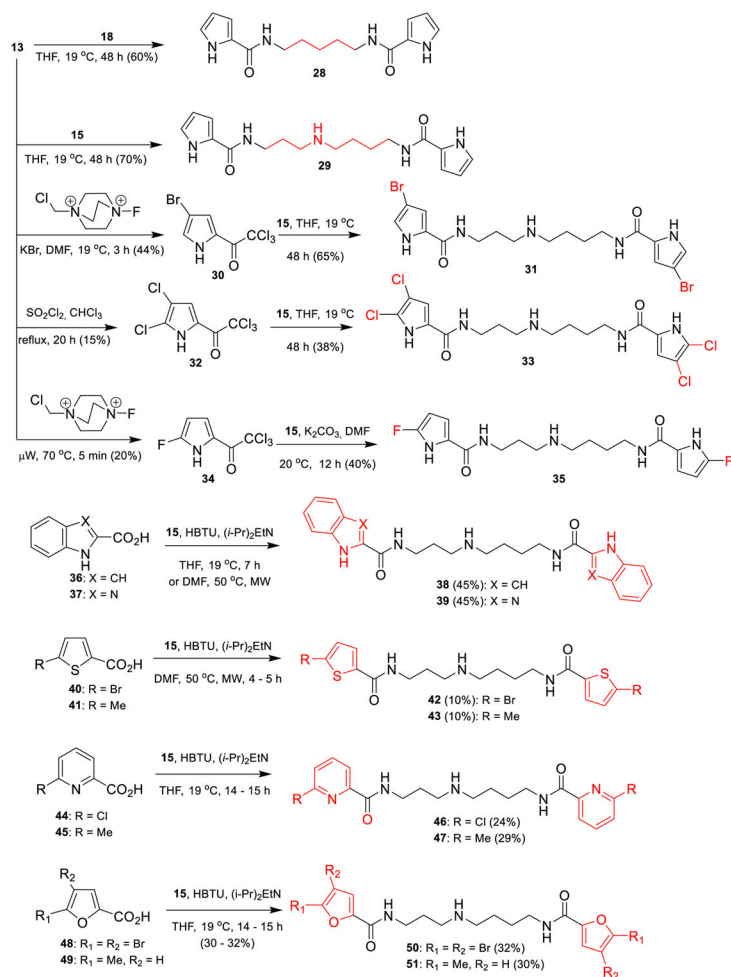


Figure 7. Isobologram plot for drug interaction analysis of pseudoceratidine (1) and sodium artesunate.



Scheme 1.
Syntheses of pseudoceratidine derivatives with variations in the tether.

**Scheme 2.**

Syntheses of pseudoceratidine derivatives with variations in the pyrrole (aromatic) moiety.

Table 1

¹H NMR Data (δ , ppm) for Pseudoceratidines 2–8 in DMSO-*d*₆

Position	2 ^b (<i>J</i> in Hz)	3 ^b (<i>J</i> in Hz)	4 ^a (<i>J</i> in Hz)	5 ^a (<i>J</i> in Hz)	6 ^b (<i>J</i> in Hz)	7 ^b (<i>J</i> in Hz)	8 ^b (<i>J</i> in Hz)
N-H	12.60, br s	12.63/12.61, s	12.18, br s	12.63, d (2.2)	n.o.	n.o.	n.o.
2							
3			6.72, dd (2.5, 2.7)				
4	6.86, m	6.88/6.87, s	6.11, dd (2.5, 3.7)	6.89, d (2.2)		6.89, s	
5							
6							
N-H	8.06, t (5.6)/8.04, m	8.10, m	8.03, t (5.7)	8.14, t (5.7)	7.76, t (6.1)	8.14, t (5.6)	7.34, br t
8	3.19, m	3.21/3.17, m	3.20, m	3.20, m	3.25, m	3.21, m	3.16, m
9	1.47/1.41, m	1.40/1.37, m	1.52, m	1.52, m	1.53, m	1.52, m	1.48, m
10	1.53/1.45, m	1.49/1.45, m	1.57, m	1.57, m	1.58, m	1.58, m	1.57, m
11	3.24/3.21, m	3.24/3.20, m	2.90, br m	2.90, br m	2.90, m	2.89, m	2.88, t (7.4)
N-H	n.o.	n.o.	n.o.	n.o.	n.o.	n.o.	n.o.
13	3.25/3.24, m	3.23/3.22, m	2.90, br m	2.90, br m	2.90, m	2.86, m	2.83, t (7.4)
14	1.73/1.64, m	1.68/1.64, m	1.77, m	1.77, m	1.79, m	1.76, m	1.73, m
15	3.17, m	3.16/3.15, m	3.25, m	3.25, m	3.29, m	3.25, m	3.20, q (6.2)
N-H	8.09, t (5.6)/8.04, m	8.10, m	8.24, t (6.0)	8.15, t (5.7)	8.24, t (5.6)	7.72, t (6.0)	7.61, t (6.0)
17							
18							
19	6.89, m	6.88/6.87, s	6.90, d (2.2)	6.13, dd (2.5, 3.7)	6.90 s		
20				6.71, dd (2.5, 2.7)			
21							
N-H	12.60, br s	12.63/12.61, s	12.67, d (2.2)	12.13, br s	n.o.	n.o.	n.o.
23		8.00/7.99, s					
24	1.97/1.94, s						

^a 400 MHz;^b 600 MHz;n.o.: not observed; ¹H signals for the HCO₂⁻ counterion observed between δ H 8.12 and 8.33 for all compounds.

Table 2

¹³C NMR Data (δ , ppm) for Pseudoceratidines 2–8 in DMSO-*d*₆

Position	2 ^b δ_c , type	3 ^b δ_c , type	4 ^a δ_c , type	5 ^a δ_c , type	6 ^b δ_c , type	7 ^b δ_c , type	8 ^b δ_c , type
2	104.6, C	104.777/104.68, C	102.7, C	104.7, C	n.o.	104.6, C	n.o.
3	97.9, C	98.09/98.07, C	111.7, CH	98.0, C	n.o.	97.9, C	n.o.
4	112.5, CH	112.8/112.6, CH	111.0, CH	112.9, CH	n.o.	112.6, CH	n.o.
5	128.4, C	128.53/128.47, C	128.4, C	128.0, C	n.o.	128.3, C	n.o.
6	158.93/159.0, C	159.2/159.15, C	159.9, C	159.4, C	n.o.	159.1, C	162.8, C
8	38.5/38.3, CH ₂	38.5/38.3, CH ₂	38.0, CH ₂	37.9, CH ₂	38.3, CH ₂	38.0, CH ₂	37.3, CH ₂
9	26.8/26.6, CH ₂	26.8/26.4, CH ₂	26.52, CH ₂	26.6, CH ₂	26.37, CH ₂	26.5, CH ₂	27.0, CH ₂
10	26.0/25.0, CH ₂	25.8/24.5, CH ₂	23.3, CH ₂	23.4, CH ₂	23.31, CH ₂	23.3, CH ₂	23.4, CH ₂
11	47.8/44.5, CH ₂	46.4/40.1, CH ₂	46.8, CH ₂	46.9, CH ₂	46.80, CH ₂	46.7, CH ₂	46.9, CH ₂
13	45.8/42.7, CH ₂	44.2/41.0, CH ₂	45.07, CH ₂	45.09, CH ₂	44.9, CH ₂	44.7, CH ₂	44.8, CH ₂
14	28.8/27.8, CH ₂	28.2/27.4, CH ₂	26.4, CH ₂	26.57, CH ₂	26.2, CH ₂	26.5, CH ₂	26.9, CH ₂
15	36.5/36.3, CH ₂	36.6/36.0, CH ₂	36.0, CH ₂	35.8, CH ₂	36.0, CH ₂	35.3, CH ₂	34.8, CH ₂
17	158.95/159.1, C	159.2/159.13, C	159.1, C	160.2, C	159.4, C	162.0, C	163.9, C
18	128.3, C	128.50/128.41, C	128.1, C	128.3, C	128.3, C	n.o.	n.o.
19	112.4, CH	112.8/112.6, CH	112.7, CH	111.1, CH	112.8, CH	n.o.	n.o.
20	97.9, C	98.09/98.07, C	98.1, C	112.0, CH	98.0, C	n.o.	n.o.
21	104.5, C	104.75/104.63, C	104.9, C	102.4, C	104.6, C	n.o.	n.o.
23	169.6/169.3, C	163.2/163.1, CH					
24	21.4/21.3, CH ₃						

^a 100 MHz;^b 150 MHz;

n.o.: not observed

Table 3¹H NMR Data (δ , ppm) for Tedamides A–D (9–12) in DMSO-*d*₆.

Position	9 ^a (J in Hz)	10 ^a (J in Hz)	11 ^b (J in Hz)	12 ^b (J in Hz)
N-H	12.63, d (1.6)	9.07, d (1.6)	n.o.	9.07, br
2				
3				
4	6.90, m	7.30, d (1.6)		7.29, s
5				
6				
N-H	8.14, t (5.7)	8.28, m	7.54, t (5.8)	8.27, t (5.9)
8	3.21, m	3.08, m	3.21, m	3.10, m
9	1.49, m	1.46, m	1.54, m	1.48, m
10	1.53, m	1.57, m	1.58, m	1.54, m
11	2.88, br	2.88, m	2.88, m	2.88, m
N-H	n.o.	n.o.	n.o.	n.o.
13	2.88, br	2.88, m	2.85, m	2.85, m
14	1.73, m	1.78, m	1.74, m	1.77, m
15	3.11, m	3.26, m	3.15, m	3.26, m
N-H	8.39, t (6.0)	8.25, m	8.39, t (5.9)	7.71, t (6.0)
17				
18				
19	7.34, d (1.7)	6.90, m	7.33, s	
20				
21				
N-H	9.09, d (1.5)	12.67, d (1.4)	9.08, br	n.o.
O-CH ₃	3.18, s	3.17, s	3.17, s	3.16, s

^a400 MHz;^b600 MHz;

n.o.: not observed

Table 4¹³C NMR Data (δ , ppm) for Tedamides A–D (9–12) in DMSO-*d*₆

Position	9 ^a δ_C , type	10 ^a δ_C , type	11 ^b δ_C , type	12 ^b δ_C , type
2	104.6, C	167.1, C	n.o.	167.3, C
3	97.9, C	92.1, C	n.o.	92.29, C
4	112.6, CH	144.5, CH	n.o.	144.73, CH
5	128.3, C	121.5, C	n.o.	121.71, C
6	159.0, C	165.6, C	160.4, C	165.8, C
8	38.0, CH ₂	38.7, CH ₂	37.9, CH ₂	38.8, CH ₂
9	26.4, CH ₂	26.1, CH ₂	26.67, CH ₂	26.1, CH ₂
10	23.2, CH ₂	23.1, CH ₂	23.3, CH ₂	23.2, CH ₂
11	46.7, CH ₂	46.6, CH ₂	46.9, CH ₂	46.7, CH ₂
13	44.7, CH ₂	44.9, CH ₂	44.9, CH ₂	44.8, CH ₂
14	25.8, CH ₂	26.3, CH ₂	25.9, CH ₂	26.6, CH ₂
15	36.5, CH ₂	35.9, CH ₂	36.6, CH ₂	35.5, CH ₂
17	166.0, C	159.3, C	166.2, C	162.0, C
18	121.6, C	128.1, C	121.79, C	n.o.
19	144.5, CH	112.8, CH	144.72, CH	n.o.
20	92.0, C	98.0, C	92.21, C	n.o.
21	167.2, C	104.8, C	167.4, C	n.o.
23	51.1, CH ₃	51.1, CH ₃	51.3, CH ₃	51.3, CH ₃

^a100 MHz;^b150 MHz;

n.o.: not observed

Table 5

Antileishmanial, Anti-*T. cruzi*, Anti-Plasmodial and Cytotoxicity Activities of Pseudoceratidine Derivatives.

Compd.	<i>L. infantum</i> promastigotes		<i>L. amazonensis</i> promastigotes		<i>T. cruzi</i> epimastigotes		Bone marrow-derived macrophages		<i>P. falciparum</i> (3D7)		HepG2	
	EC ₅₀ ±S.D. (µM)	EC ₅₀ ±S.D. (µM)	EC ₅₀ ±S.D. (µM)	EC ₅₀ ±S.D. (µM)	EC ₅₀ ±S.D. (µM)	EC ₅₀ ±S.D. (µM)	CC ₅₀ ±S.D. (µM)	EC ₅₀ ±S.D. (µM)	EC ₅₀ ±S.D. (µM)	MDL ₅₀ ±S.D. (µM)	MDL ₅₀ ±S.D. (µM)	Selectivity Index ^a
1	>100	>100	>100	>100	>100	-	-	1.1 ± 0.1 (0.96 – 1.24)	16 ± 1 (14.6 – 17.4)	-	-	15
2	>100	>100	>100	>100	>100	-	-	>10	-	-	-	-
4+5	>100	>100	>100	>100	>100	-	-	5.8 ± 0.5 (5.11 – 6.49)	400	-	-	69
9+10	>100	>100	>100	>100	>100	-	-	>100	-	-	-	-
16	>100	>100	>100	>100	>100	-	-	4 ± 1 (3 – 6)	160 ± 23 (128 – 192)	-	-	35
17	>100	>100	>100	>100	>50	-	-	>10	-	-	-	-
20	24 ± 3 (20 – 27)	19 ± 1 (18 – 20)	7 ± 1 (5 – 7)	52 ± 3 (49 – 55)	>100	-	-	>10	-	-	-	-
21	>100	>100	>100	>100	>100	-	-	>10	-	-	-	-
23	19 ± 1 (17 – 20)	44 ± 5 (38 – 49)	>100	>100	>100	>100	>100	2 ± 1 (0.20 – 3)	99 ± 12 (82 – 116)	-	-	52
25	>100	>100	>100	>100	>100	-	-	2 ± 1 (2 – 3)	263 ± 43 (203 – 323)	-	-	101
27	24 ± 3 (21 – 28)	43 ± 2 (41 – 45)	24 ± 4 (21 – 27)	66 ± 5 (61 – 72)	>100	-	-	>10	-	-	-	-
28	>100	>100	>100	>50	>50	-	-	>10	-	-	-	-
29	>100	>100	>100	>100	>100	-	-	>10	-	-	-	-
31	>100	>100	>100	>100	>100	-	-	7 ± 1 (6 – 8)	400	-	-	54
33	>100	>100	>100	>100	>100	-	-	>10	-	-	-	-
35	>100	>100	>100	>100	>100	-	-	>10	-	-	-	-
38	>100	>100	>100	>100	>100	-	-	>10	-	-	-	-
39	>100	>100	>100	>100	>100	-	-	>10	-	-	-	-
42	20 ± 3 (17 – 24)	76 ± 2 (72 – 80)	>100	>100	>100	>100	>100	>10	-	-	-	-
43	>100	>100	>100	>100	>100	-	-	>10	-	-	-	-
46	>100	>100	>100	>100	>100	-	-	>10	-	-	-	-

	<i>L. infantum</i> promastigotes	<i>L. amazonensis</i> promastigotes	<i>T. cruzi</i> epimastigotes	Bone marrow-derived macrophages	<i>P. falciparum</i> (3D7)	HepG2	
Compd.	EC ₅₀ ±S.D. (μM)	EC ₅₀ ±S.D. (μM)	EC ₅₀ ±S.D. (μM)	CC ₅₀ ±S.D. (μM)	EC ₅₀ ±S.D. (μM)	MDL ₅₀ ±S.D. (μM)	Selectivity Index ^a
47	>100	>100	>100	-	>10	-	-
50	23 ± 5 (17 – 28)	18 ± 2 (16 – 19)	>100	82 ± 4 (78 – 87)	3 ± 1 (2 – 4)	400	125
51	>100	>100	>100	-	>10	-	-

EC₅₀: half maximal effective concentration; CC₅₀: half maximal cytotoxic concentration; S.D.: standard deviation; 95% confidence interval values are shown in parentheses; -: not determined;

^aSelectivity index: MDL₅₀/IC₅₀ for *P. falciparum*.

Table 6

Antiplasmodial Activities of Pseudoceratidine (1) and Standard Antimalarials Against Sensitive (3D7 strain) and Resistant *P. falciparum* (K1 strain).

Compound	<i>P. falciparum</i> IC ₅₀ (μM)	
	3d7 strain	K1 strain
Pseudoceratidine (1)	1.1 ± 0.1	1.1 ± 0.1
Chloroquine	0.013 ± 0.002	0.167 ± 0.002
Pyrimethamine	0.03 ± 0.01	3.9 ± 0.1
Cycloguanil	0.010 ± 0.002	0.54 ± 0.02
Artesunate	0.004 ± 0.001	0.003 ± 0.001